Neuropharmacology 218 (2022) 109210

Contents lists available at ScienceDirect

Neuropharmacology

journal homepage: www.elsevier.com/locate/neuropharm

Role of Perineuronal nets in the cerebellar cortex in cocaine-induced conditioned preference, extinction, and reinstatement

Julian Guarque-Chabrera, Aitor Sanchez-Hernandez, Patricia Ibáñez-Marín, Ignasi Melchor-Eixea, Marta Miquel *

Área de Psicobiología, Universitat Jaume I, Facultat de Ciencies de la Salut, Avenida Vicente Sos Baynat sn, 12071, Castellón de la Plana, Spain

ARTICLE INFO

Keywords:
Perineuronal nets
Cerebellum
Chondroitinase ABC
Addiction
Cocaine

ABSTRACT

Perineuronal nets (PNNs) are cartilage-like structures of extracellular matrix molecules that enwrap in a net-like manner the cell-body and proximal dendrites of special subsets of neurons. PNNs stabilize their incoming connections and restrict plasticity. Consequently, they have been proposed as a candidate mechanism for drug-induced learning and memory. In the cerebellum, PNNs surround Golgi inhibitory interneurons and both inhibitory and excitatory neurons in the deep cerebellar nuclei (DCN). Previous studies from the lab showed that cocaine-induced conditioned memory increased PNN expression in the granule cell layer of the posterior vermis. The present research aimed to investigate the role of cerebellar PNNs in cocaine-induced conditioned preference. For this purpose, we use the enzyme chondroitinase ABC (ChABC) to digest PNNs at different time points of the learning process to ascertain whether their removal can affect drug-induced memory. Our results show that PNN digestion using ChABC in the posterior vermis (Lobule VIII) did not affect the acquisition of cocaine-induced conditioned preference. However, the removal of PNNs in Lobule VIII -but not in the DCN- disrupted short-term memory of conditioned preference. Moreover, although PNN digestion facilitated the formation of extinction, reinstatement of cocaine-induced conditioned preference was encouraged under PNN digestion. The present findings suggests that PNNs around Golgi interneurons are needed to maintain cocaine-induced Pavlovian memory but also to stabilize extinction memory. Conversely, PNN degradation within the DCN did not affect stability of cocaine-induced memories. Therefore, degradation of PNNs in the vermis might be used as a promising tool to manipulate drug-induced memory.

1. Introduction

Perineuronal nets (PNNs) are mesh-like structures of extracellular matrix molecules (ECM), such as hyaluronan, chondroitin sulfate proteoglycans (CSPGs), link proteins, and tenascins that wrap the cell-body and proximal dendrites of special subsets of neurons (Carulli et al., 2006; Dauth et al., 2016; Giamanco and Matthews, 2012; Slaker et al., 2016). The majority of PNNs are found surrounding fast-spiking parvalbumin+ (PV+) GABAergic interneurons (Celio and Chiquet-Ehrismann, 1993; Hartig et al., 1992; Kosaka and Heizmann, 1989). However, they are also present around excitatory neurons (Morikawa et al., 2017; Wegner et al., 2003). In the cerebellum, PNNs surround Golgi GABAergic interneurons and Lugaro cells in the cerebellar cortex and both excitatory and inhibitory neurons in the DCN (Carulli et al., 2006, 2020; Corvetti and Rossi, 2005; Crook et al., 2007).

Emergence of PNNs correlates with developmental critical periods, synaptic refinement, and myelination to restrict juvenile plasticity and regulate adult synaptic plasticity processes (Dityatev et al., 2007; Pizzorusso et al., 2002). PNNs stabilize incoming connections and restrict plasticity (Corvetti and Rossi, 2005; Foscarin et al., 2011; Lensjø et al.,

Abbreviations: PNNs, Perineuronal nets; ChABC, chondroitinase ABC; DCN, Deep Cerebellar Nuclei; Acq, Cocaine-induced Memory Acquisition; Ret, Cocaine-induced Short-Term Memory; Ext, Extinction of Cocaine-induced Memory; Reins, Reinstatement of Cocaine-induced Memory; ECM, Extracellular Matrix Molecules; CSPGs, Chondroitin Sulfate Proteoglycans; PV, Parvalbumin; SUD, Substance Use Disorder; Med, Medial Deep Nucleus of the Cerebellum; Int, Interposed Deep Nucleus of the Cerebellum; Lat, Lateral Deep Nucleus of the Cerebellum; CS+, Cocaine-associated stimulus; CS-, Saline-associated stimulus; WFA, *Wisteria floribunda agglutinin*; GCL, The granule cell layer; AU, Arbitrary Units; OV, Overlap; KDE, Kernel Density Estimation; PS, Probability of Superiority; CI, Confident Interval; MMPs, Metalloproteinases.

* Corresponding author.
E-mail address: miquel@uji.es (M. Miquel).

https://doi.org/10.1016/j.neuropharm.2022.109210
Received 20 May 2022; Received in revised form 31 July 2022; Accepted 2 August 2022
Available online 17 August 2022

2017a, 2017b; Pizzorusso et al., 2002), and because of the stability of their components, they have been proposed as a key mechanism through which drug-induced long-lasting memories could be maintained (Sorg et al., 2016). Preclinical studies have shown that drug-induced conditioned preference (Blacktop et al., 2017; Carbo-Gas et al., 2017; Gil-Miravet et al., 2019; Guarque-Chabrera et al., 2022; Jorgensen et al., 2020; Slaker et al., 2015; Traver et al., 2019; Xue et al., 2014), drug self-administration (Blacktop et al., 2017; Blacktop and Sorg, 2019; Chen et al., 2015; Coleman et al., 2014; Roura-Martínez et al., 2020; Sanchez-Hernandez et al., 2021; Vazquez-Sanroman et al., 2017), and drug withdrawal (Roura-Martínez et al., 2020; Sanchez-Hernandez et al., 2021; Van Den Oever et al., 2010; Vazquez-Sanroman et al., 2015a, 2015b) regulate PNN expression in different brain regions, including the cerebellum.

Although the traditional role of the cerebellum was mainly linked to motor control, increasing evidence in the last two decades has pointed to its involvement in a broader spectrum of brain functions such as reinforcement learning (Carta et al., 2019; Kostadinov and Häusser, 2022; Wagner et al., 2017), aversive learning (Frontera et al., 2020; Sacchetti et al., 2005), and executive functions (Deverett et al., 2019). Direct and indirect reciprocal connectivity between the cerebellum and other brain regions can explain these unexpected cerebellar roles. In particular, the cerebellum modulates activity in the medial prefrontal cortex (Chen et al., 2014; Forster and Blaha, 2003; Gil-Miravet et al., 2021), limbic regions (Frontera et al., 2020; Sacchetti et al., 2005), basal ganglia (Bostan and Strick, 2018), striatum (Chen et al., 2014), and VTA (Carta et al., 2019; Gil-Miravet et al., 2021). Dysfunction of all these regions underlie substance use disorder (SUD) and other neuropsychiatric disorders that exhibit comorbidity with SUD (Miquel et al., 2019).

Studies of cue reactivity in patients with SUD have shown cerebellar activation when drug-related cues are presented (for a review see Moulton et al., 2014; Moreno-Rius and Miquel, 2017). Preclinical studies from our lab evidenced increased neural activity in granule cells and PNN expression around Golgi interneurons (Carbo-Gas et al., 2014a, 2017). Remarkably, these cerebellar signatures were exclusive of those animals that expressed conditioned preference towards cocaine-related cues and correlated with the expression of drug-induced conditioned preference in lobules VIII and IX, ruling out the possibility that cerebellar activity results from unconditioned stimulating properties of cocaine or movements performed during the test. Moreover, an infralimbic deactivation not only facilitated the acquisition of cocaine-related memory but also increased the expression of PNNs around Golgi interneurons in these posterior medial lobules (VIII and IX) (Guarque-Chabrera et al., 2022).

Broadly used to digest PNNs is the bacterial enzyme chondroitinase ABC (ChABC). ChABC digests the chondroitin sulfate glycosaminoglycans of the CSPG and the hyaluronan (Brückner et al., 1998; Fox and Caterson, 2002; Prabhakar et al., 2005), disrupting the macromolecular PNN arrangement and promoting neuronal plasticity (Corvetti and Rossi, 2005; Pizzorusso et al., 2002). ChABC has been used to investigate the role of PNNs in drug addiction. Removal of PNNs in the amygdala promotes extinction of drug-related memories (Xue et al., 2014), disrupted cocaine-induced conditioning in the prelimbic (PL) (Slaker et al., 2015), and reduced cocaine-self administration in the anterior hypothalamic area (Blacktop et al., 2017; Blacktop and Sorg, 2019). Therefore, PNN digestion may be a promising strategy to manage the over-consolidated drug-related Pavlovian memories that lead to relapse.

Here, we sought to investigate the role of cerebellar PNNs in the formation, short-term memory, extinction and reinstatement of drug-induced conditioned memories. We focused on lobule VIII given that our previous research pointed to neuronal activity and PNN expression in this lobule as highly correlated to the expression of cocaine-induced conditioned preference. For this purpose, we use the enzyme ChABC to digest PNNs at various time points of the learning process to ascertain whether their degradation can affect drug-induced memories.

2. Materials and methods

The National Centre for the Replacement, Refinement and Reduction of Animals in Research (NC3Rs) has published in 2010 the ARRIVE (Animals in Research: Reporting In Vivo Experiments) guidelines (Kilkenny et al., 2010) that had been recently updated as ARRIVE 2.0 (Percie du Sert et al., 2020a, 2020b). These guidelines consist in a 20-item checklist of 10-essential (basic in a manuscript) and 10-recommended (to add context to the study) items that need to be included in a manuscript to promote transparency, rigorousness, and reproducibility of animal research. We complied with the guidelines and as they recommend, we also created flowcharts to illustrate every step we took on each experiment (appendixes A and B).

2.1. Subjects

The present study includes 67 male Sprague-Dawley rats (Janvier, ST Berthevin Cedex, France). Rats arrived at the animal facilities (Jaume I University, Spain) weighing ~125 (~P28) and ~225 (~P38) g. The rationale of using animals of two different ages was based on both the requirements for stereotaxic surgery and the necessity to terminate the different experiments with animals having similar ages (>P63, young adults) to be able to compare between conditions.

Then, rats were housed individually with temperature and humidity controlled and under standard conditions in a 12-h light-dark cycle (from 8:00 a.m. to 8:00 p.m.), with access to food and water *ad libitum*. Before the experiments started rats were handled for 2 days. Animal procedures were approved by the local Animal Welfare Ethics Committee and Empowered Body (2014/VSC/PEA/00208; 0139) and adhered to the European Community Council directive (2010/63/EU), Spanish directive (BOE 34/11370/2013), and local directive (DOGV 26/2010).

2.2. Pharmacological agents

Cocaine hydrochloride (Alcaliber S.A., Madrid, Spain) was dissolved in a 0.9% saline solution and administered intraperitoneally (IP). Saline solution was used as a control vehicle. Anesthesia was induced using a cocktail of ketamine (100 mg/kg) (Ketamidor 50 mL, 100 mg/mL; Richterpharma AG, Wels, Austria), and xylazine (10 mg/kg) (Xylazine hydrochloride ≥99% (HPLC); CAT# X1251; Sigma-Aldrich, Madrid, Spain) or anesthetized with isoflurane (1000 mg/g) (Isoflutek 250 ml, Laboratorios Karizoo S.A., Barcelona, Spain) (induction at 3.00% and maintenance through the whole surgery at 2.00%) using a Isotec 5 isoflurane anesthesia vaporizer (Datex-Ohmeda Inc., Madison, WI). PNN digestion was achieved by intracranial infusions of 25 U/mL of the enzyme ChABC (Chondroitinase ABC from Proteus vulgaris BSA free; CAT# C3667; Sigma-Aldrich, Madrid, Spain) dissolved in aqueous 0.01% BSA (Bovine Serum Albumin cold ethanol fraction, pH 5.2, ≥96%; CAT# A4503; Sigma-Aldrich, Madrid, Spain).

2.3. Stereotactic surgery and enzymatic digestion

The Rat Brain in Stereotaxic Coordinates (Paxinos and Watson, 1998) atlas were used to calculate the coordinates for our enzymatic digestions. In the experiment 1 in which we performed the infusions before conditioning, we used older animals (arrival: ~225g (~P38)) that received the surgery weighing ~270 g (~P45). In those experiments in which the animals were conditioned before receiving the enzymatic digestion, experiments 2–4, we accounted for the weight gains of the rats through the time prior to the surgery, so we started the training with younger animals (arrival: ~125 g (~P28); training start: ~175 g (~P35)) that received the surgery weighing ~350 g (~P53).

Rats were anesthetized with a cocktail of ketamine/xylazine or isoflurane and placed in a stereotaxic apparatus (Kopf Model 902; David Kopf Instruments, Tujunga, CA, USA). A small craniotomy was

performed using a 0.9 mm drill bit (Burrs for Micro Drill; CAT# 19008–09; Fine Science Tools, Heidelberg Germany). Intracranial infusions were performed by placing a stainless steel guide cannula (23-gauge external diameter) in the posterior vermis (medial cerebellum) (lobule VIII; LVIII) (AP: −14.5; ML: 0; DV: −4.5) (Figs. 2B, 3B and 5B), or in the DCN, the medial (Med) (AP: −11.4; ML: ±1; DV: −6), the interposed (Int) (AP: −11.3; ML: ±2.5; DV: −5.8), and the lateral (Lat) (AP: −11.4; ML: ±3.6; DV: −6.2) nuclei (Fig. 4B) (Paxinos and Watson, 1998). Then, a removable stainless steel injector (30-gauge external diameter) connected to a 10 μl Hamilton syringe (Microliter Syringe Model 701 N; Cat# 80300; Hamilton Bonaduz AG, Bonaduz, Switzerland) was inserted into the previously placed guide cannula, and 1 μL of ChABC (25 U/mL) or vehicle (aqueous 0.01% BSA; sham group) were infused (0.50 μL/min) into the targeted area using an infusion pump (11 Plus dual Syringe; Cat# HA702209; Harvard Appatarus, Holliston, MA, USA). After the infusion was completed, the injector remained in place for 3 min to allow for proper diffusion and to avoid liquid aspiration. Then, the guide cannula and injector were removed and the wound was sutured. Rats were left undisturbed for four days after surgery for recovery and received analgesic treatment with meloxicam (Metacam 20 mL, 5 mg/mL; Boehringer Ingelheim, Barcelona, Spain) every 24 h for two days.

2.4. Behavioral protocols

All protocols involving animals took place within the first 5 h of their light cycle, 2 h after the lights were turned on. All behavioral procedures were conducted in a black opaque corridor (90 × 20 × 60 cm) containing three equal chambers (30 × 20 × 60 cm). One day before the conditioning training, animals were habituated to the apparatus in a 30-min session without the olfactory cues used as CS+/CS-. For conditioning (Fig. 1A), extinction (Fig. 1D), and reinstatement (Fig. 1E), two equally preferred olfactory cues, lavender or rose, were used as CS+/CS- (Guarque-Chabrera et al., 2022). Two drops of lavender or rose fragrance were put on gauze and presented inside a steel ball with holes that hung on the walls of the two lateral chambers (Fig. 1).

2.4.1. Conditioning

To test the effect of enzymatic digestion of PNNs on the acquisition of cocaine-induced memory, animals received ChABC or vehicle infusions in the posterior cerebellar vermis (LVIII) five days before the initiation of conditioning (Fig. 2A–C). Then, the scents were associated with cocaine (10 mg/kg) or saline injections (IP), acting as CS+ and CS- respectively (Fig. 1C). For each pairing session, rats were confined in one of the lateral chambers of the apparatus for 15 min with one of the olfactory cues (Fig. 1A). Eight cocaine- and eight saline-paired sessions were conducted on alternate days (Fig. 1C). A preference test was

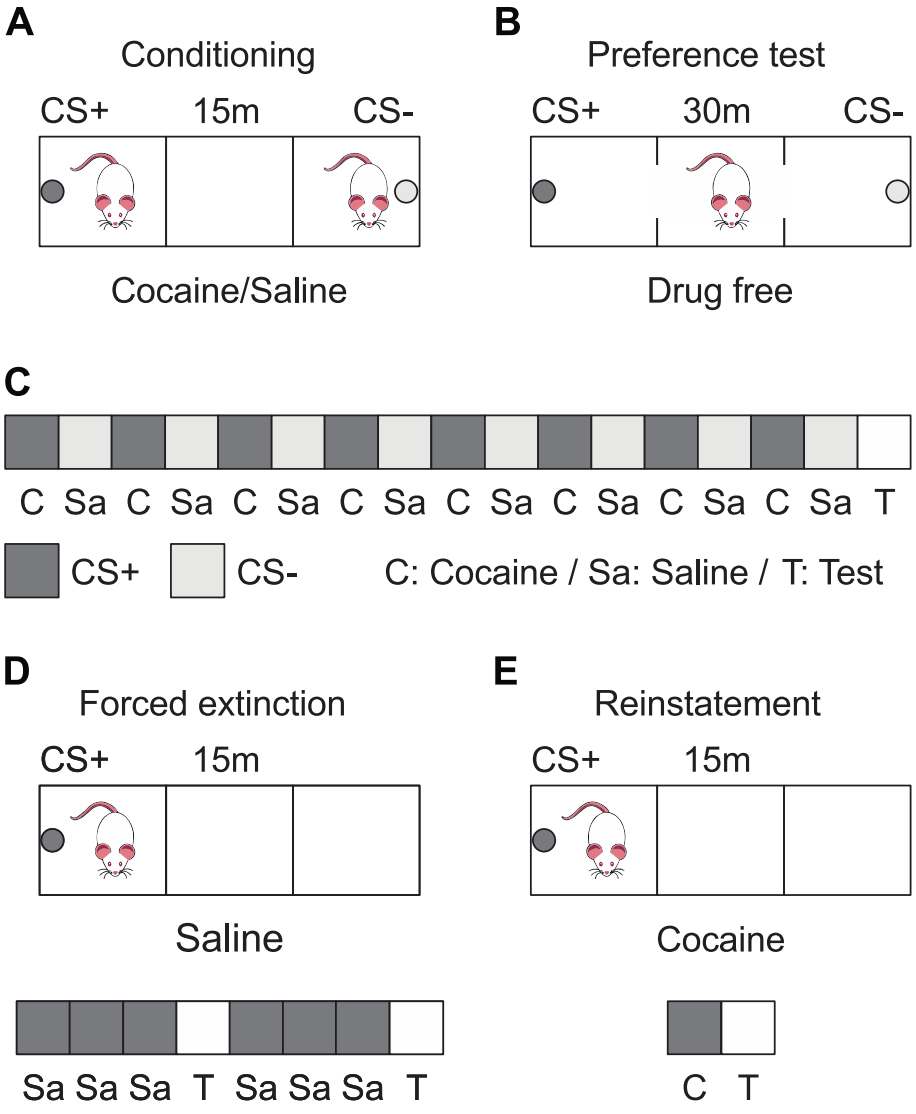

Fig. 1. Schematics of behavioral paradigms and cocaine/saline administration schedules. (**A**) Representation of the corridor for conditioning. Animals were confined in one of the lateral chambers of the apparatus for 15 min with one of the olfactory cues (lavender or rose) for each pairing session. Eight CS+ (dark gray) cocaine- and eight CS- (light gray) saline-paired sessions were conducted on alternate days. (**B**) Layout in the preference test. (**C**) Distribution of the cocaine/saline administration schedule for conditioning. (**D**) Top schematic depicts the layout during forced extinction training. Rats were confined in one of two compartments in the presence of CS+ (top) and saline was administered as represented in the bottom schedule. (**E**) For reinstatement, conditioned memory was reactivated by a cocaine injection (10 mg/kg) in the presence of the CS+ (bottom) 24 h before the preference test (bottom). C: Cocaine; Sa: Saline; T: Test.

carried out 48 h after the last cocaine administration (Figs. 1C and 2A). Olfactory cues and their locations in the lateral arms were counterbalanced between animals.

2.4.2. Preference test

In order to prevent any cue but the olfactory ones to guide behavior, the apparatus was rotated 90° from its original position and rats were placed in the central chamber. Rats were free to move throughout the three chambers of the corridor in a 30-min drug-free test in which CS+ and CS− olfactory cues were presented simultaneously, one on each opposite lateral arm of the corridor (Fig. 1B). All the test sessions were videotaped and scored by a blind observer. The first 10 min were not considered in order to allow the animal to explore the new location of the olfactory cues. Preference score was calculated as [Time Spent in CS+/((Time Spent in CS+) + (Time Spent in CS−))] × 100.

2.4.3. Short-term memory

We infused ChABC or vehicle into LVIII (Fig. 3A) or the DCN (Fig. 4A) after the acquisition (Acq) test. Following 4 days of ChABC infusion, we conducted another preference test (Ret) to assess short-term memory of cocaine-induced conditioned preference.

2.4.4. Extinction

To test the effects of PNN removal on extinction, we used a forced extinction procedure (Fig. 1D). Twenty-four hours after the Acq test, animals underwent surgery to receive ChABC or vehicle infusions in LVIII (Fig. 5A–C). Only those rats showing preference for the CS+ >50% were infused with ChABC/vehicle and underwent extinction training. Four days after surgery, rats received saline injections and were confined with the CS+ in one of the lateral chambers. Every three CS + -saline pairings, rats were tested for their conditioned preference. Extinction training lasted a total of 6 saline parings and 2 preference tests (Ext1, Ext2) (Fig. 1D).

2.4.5. Reinstatement

After forced extinction, rats were left undisturbed for 8 days in their home cages and another preference test was carried out to assess the duration of extinction (ExtLT) (Figs. 1E and 5A). Then, rats received a cocaine injection (10 mg/kg, IP) and were immediately confined in one of the lateral chambers with the CS + for 15 min (Fig. 1E). The next day, a new preference test (Reins) was performed to assess reinstatement of the original cocaine-cue association (Figs. 1B and 5A).

2.5. Perfusion protocol and brain sampling

All animals were perfused transcardially 90 min following the last preference test on each behavioral protocol. Rats were deeply anesthetized with sodium pentobarbital (30 mg/kg) (Dolethal 100 mL, Vetoquinol E.V.S.A., Madrid, Spain) and perfused using first saline (0.9%) with heparin (0.006%) (Heparin sodium salt from porcine intestinal mucosa; CAT# H3393; M Sigma-Aldrich, Madrid, Spain) and then paraformaldehyde (4%) (Paraformaldehyde, powder, 95%; CAT# 158127; M Sigma-Aldrich, Madrid, Spain). Cerebella were extracted and stored with the same fixative for 24 h at room temperature. Then, the tissue was immersed in sucrose solution (30%) with sodium azide (2%) (Sodium azide BioXtra; Cat# S8032; Sigma-Aldrich, Madrid, Spain) until the brain sank at 4 °C. Brain tissue was covered them with Neg-50™ (Richard Allan Scientific Neg 50™; Cat# 6502; Thermo Fisher Scientific, Barcelona, Spain) and fast frozen by immersion in liquid nitrogen. Then, four series of sagittal (the posterior cerebellar cortex) or coronal (the DCN) sections of the cerebellum were performed at 40 μm with a cryostat microtome (Microm HM560, Thermo Fisher Scientific, Barcelona, Spain) and were stored at −20 °C in cryoprotectant solution.

2.6. Immunofluorescence labeling

The degree of enzymatic digestion using ChABC was determined by *Wisteria floribunda agglutinin* (WFA) immunolabeling on free-floating sections. Sagittal sections of the cerebellum were selected according to the lateral coordinates from −0.72 to 0.72 mm, comprising the whole vermis (Paxinos and Watson, 1998). ChABC digestion in the DCN was determined in coronal sections of the cerebellum and brainstem according to the coordinates −10.52 to −11.80 mm from bregma, comprising the whole DCN (Paxinos and Watson, 1998). After several rinses with phosphate-buffer saline with 0.1 M Triton X-100 (1%) (Cat# T9284; Sigma-Aldrich, Madrid, Spain) (PBST), cerebellar sections were incubated overnight at 4 °C with biotinylated WFA (1:200; Lectin from *Wisteria floribunda*; CAT# L1516; Sigma Aldrich, Madrid, Spain), which binds to the glycosaminoglycan chains of the proteoglycans that form the PNN structure (Hartig et al., 1992), dissolved in PBST. The next day, and after several rinses, tissue was incubated in PBST using Cy3-streptavidin (1:200; CAT# 016-160-084; Jackson Immunoresearch Europe Ltd, Suffolk, UK) for 120 min at room temperature. Once fluorescence reaction occurred, cerebellar sections underwent several rinses and were mounted using Mowiol (Calbiochem, Merck Chemicals and Life Science, Madrid, Spain), and stored at 4 °C until imaging.

2.7. Image acquisition and analysis

The effects of ChABC on cerebellar PNNs were assessed within the apical region of the granule cell layer (GCL) in LVIII of the vermis (Fig. 2F–H, 3F, 5F), and in the DCN (Fig. 4F). Tile-scan (3 × 3) Z-stack images (25 steps) were acquired using a confocal microscope (Leica DMi8, Leica Microsystems CMS GmbH, Wetzlar, Germany), with a 20× objective, a zoom of 2, and 2048 × 2048 px. Laser intensity (1%), gain (650), and offset (−1) were maintained constant in each acquisition. Leica Application Suite X (LAS X, Leica Microsystems CMS GmbH, Wetzlar, Germany) was used to perform a maximal projection of the tile-scan Z-stacks. Animals with digestion misplacement were not included in the statistical analysis. Image analyses were performed blindly using FIJI free software (Schindelin et al., 2012). We quantified WFA intensity (brightness range 0–255; data expressed as arbitrary units of intensity, AU of intensity) in two different ways. For general ECM assessment, we measured WFA intensity by drawing a square ROI in the dorsal region of the GCL (avoiding the white matter) (Figs. 2I, 3G and 5G) and in the DCN (Fig. 4G). To analyze WFA intensity within the PNN, we randomly selected 15 pixels in the net surrounding the soma (Figs. 4I and 5I) and calculated the average intensity of 10 PNNs in the GCL or 20 PNNs in the DCN per animal (Carbo-Gas et al., 2017; Carulli et al., 2020; Foscarin et al., 2011; Sanchez-Hernandez et al., 2021; Vazquez-Sanroman et al., 2015a). Then, the proportion of weak (0–85 AU of intensity), medium (86–170 AU of intensity), and strong (more intense) (171–255 AU of intensity) PNNs was estimated on the Sham and ChABC groups when possible.

2.8. Experimental design and statistics

One of the reasons that has led the scientific community into a reproducibility and replicability Wasserscrisis is the misuse of p values when using null hypothesis significance testing (frequentist statistics) (Anderson, 2019; Greenland et al., 2016; Nuzzo, 2014; Wasserstein and Lazar, 2016; Zingg et al., 2020). To overcome the issues derived from null hypothesis rejection based on $p < 0.05$, estimation statistics, also known as "the new statistics" (Cumming, 2012; Cumming and Calin-Jageman, 2017), focuses on the magnitude of the effect (the effect size) (Cohen, 1988) and its precision/uncertainty (confidence intervals, CI) (Altman et al., 2000). This encourages to gain a deeper understanding of the metrics used, and how they relate to the natural processes being studied. Moreover, CIs not only provide a 95% chance of covering the underlying population mean but also, they are 83%

prediction intervals (chance of covering any future experiment's mean) (Cumming and Maillardet, 2006). Consequently, we focused the report of our statistical analyses on description, effect sizes estimations, and the estimation of their uncertainty (95% confidence intervals), rather than statistical significance (we also reported *p* values) (Bernard, 2019; Calin-Jageman, 2018; Calin-Jageman et al., 2019; Ho et al., 2019).

Sample size was calculated using G*Power (Heinrich Heine University Dusseldorf, North Rhine-Westphalia, Germany) (Faul et al., 2007). We first calculated the effect size of a previously published research (Guarque-Chabrera et al., 2022) resulting in an effect size of 1.80 (Cohen's *d*). Then, establishing 5% type I error and 20% type II error rates for an $\alpha = 0.05$ and power of 80%, and using the estimated effect size for two experimental groups, we obtained a total sample size of 12 animals, resulting in a minimum of 6 animals per group. We have two experimental groups that received the same dose and cocaine schedules. The ChABC group ($N = 33$) underwent enzymatic digestion of cerebellar PNNs, while the Sham group (the control group; $N = 34$) underwent the same surgery procedure but received vehicle infusions instead.

All statistical analyses were performed using R Statistical language (version 4.1.2; R Core Team, 2021). Even though Shapiro-Wilk tests yielded normality on our data, we preferred to use non-parametric statistics/distribution-free methods to analyze the data. These estimations make fewer assumptions about the nature of the distributions, are robust with samples $n < 20$, and can be used to analyze both categorical or continuous data.

First, we used the function *hdpbci* (bootstrap, 5000 reshuffles) of the *rogme* package (Rousselet et al., 2017) to estimate the median (*Mdn*) of our groups. Then, to compare the magnitude of preference for the CS+ and WFA intensity between the two groups, we used the functions *shifthd_pbci* (for independent groups; bootstrap, 5000 reshuffles) and *shiftdhd_pbci* (for matching pairs; bootstrap, 5000 reshuffles) of the *rogme* package to assess for differences between the medians of two groups, the magnitude of this differences ($\Delta_{Mdn} = Mdn_1 - Mdn_2$) (Baguley, 2009; Ho et al., 2019; Michel et al., 2020), and their 95% confident intervals (CIs) to report the effect sizes. These functions of the *rogme* package use the Harrell-Davis quantile estimator with a percentile bootstrap approach to calculate any decile and the between-groups/within-group differences of the decile of interest. As a result, when the zero value is not included in the CIs the difference is considered statistically significant at an alpha threshold of 0.05 and without being concerned about the Type I error, in a frequentist sense. In our case, we estimated the decile 5, which corresponds to the median, the difference between the medians of two groups, and their corresponding 95% CIs. We used the function *p.adjust* from the *stats* package to correct the significance level by adjusting for multiple comparisons using the FDR method (Benjamini and Hochberg, 1995).

Next, we analyzed our experimental groups at a distribution level. First, we used the function *boot.overlap* (bootstrap, 5000 reshuffles) of the *overlapping* package (Pastore, 2018; Pastore and Calcagnì, 2019) to calculate the kernel density estimation (KDE) of two distributions and the overlap (*OV*) between them. This function estimates the area intersected by two probability density functions and is a measure of how similar two distributions are. This estimate is a distribution-free index that can be used with any kind of distribution and even in the presence of multimodality. Then, we used the function *cidv2* of the *rogme* package to obtain the probability of superiority (*PS*) between two distributions and its 95% CI. This is the probability that when randomly sampling a score from each of two groups, the observation from the second group will be larger than the observation from the first group (Ruscio, 2008). Both indexes, *OV* and *PS*, will be reported as a % with their corresponding 95% CI.

In the cases in which we had repeated measures (successive tests) to assess the preference for the CS+, we performed Sign tests to assess the direction of the change as the proportion of animals that increased or decreased their preference score between two tests. First, we used the function *binom.test* of the *mosaic* package (Pruim et al., 2017) to assess whether the proportion of success (proportion of decreased scores) within each group is different than chance (0.5). Subsequently, we used the function *prop_test* of the *rstatix* package (Kassambara, 2021) to estimate differences in the proportions of change between groups. This function returns a chi-squared test (χ^2) estimation and the CI of the difference of the success proportions between both groups. We used these CIs and the magnitude of the difference between these proportions ($\Delta_{Chi} = Pr_1 - Pr_2$) as the effect size.

We also used χ^2 to evaluate the frequency distribution of weak, medium, and strong PNNs (Carbo-Gas et al., 2017; Carulli et al., 2020; Foscarin et al., 2011; Sanchez-Hernandez et al., 2021; Vazquez-Sanroman et al., 2015a, -2015b) between the Sham and the ChABC group, as it has been shown that stronger PNNs might represent the maintenance mechanism of drug-related memory. To calculate the χ^2 with two degrees of freedom we used the function *chisq_test* of the *rstatix* package. Then, we performed post hoc comparison by using the function *prop_test* of the *rstatix* package and calculated the difference between the proportions of PNNs on each category between groups, obtaining the effect sizes ($\Delta_{Chi} = Pr_1 - Pr_2$) and their 95% CIs.

Finally, as an approach to modelling the relationship between the preference for cocaine cues and ECM and PNN expression, we used Spearman's rank correlation coefficient (*rho*). Before calculating the correlations, and since the ECM/PNN expression in both groups is very different, we normalized the preference scores and the WFA intensity scores (min-max normalization between 0 and 1 using the formula $x' = (x\text{-min}(x))/((\max(x)\text{-min}(x))$; this preserves the relationships of the original variables while converting them to a common scale) to facilitate the visualization of the data. We used the functions *cor.test* of the *stats* package (R Core Team, 2021) and *spearmanRho* of the *rcompanion* package (Mangiafico, 2022) to calculate *rho* with its 95 %CI (bootstrap, 5000 reshuffles) and the exact *p* value.

Descriptive statistics for each group will be reported as *Mdn* [95% CI]. Statistical analysis results comparing two groups will be reported as effect size ($\Delta_{group1\text{-}group2}$ = difference between medians [95% CI]) and exact *p* value, $OV_{group1\text{-}group2}$ = % of overlap [95% CI], $PS_{group1\text{-}group2}$ = % of superiority [95% CI], and χ^2 estimate (and post hoc comparisons in case of more than 1 degree of freedom) with its effect size ($\Delta_{group1\text{-}group2}$ = difference between proportions [95% CI]) and exact *p* value, and *rho* [95% CI] with its exact *p* value.

3. Results

3.1. PNN removal in lobule VIII did not affect the acquisition of cocaine-induced conditioned preference

The enzymatic digestion of PNNs in the cerebellar cortex prior to cocaine-induced preference conditioning (Fig. 2) resulted in a median preference score of 67.19 [55.70, 81.09] for the ChABC ($n = 7$) group and a score of 59.36 [50.3, 68.31] for the Sham group ($n = 8$). A test comparing both medians yielded an effect size of −7.83 [–24.59, 6.66] ($\Delta_{Sh\text{–}Ch}$) and a *p* value of 0.3416 (Fig. 2C). Then, we analyzed both groups at the distribution level. We observed that their distributions overlapped 59 [27, 92] % (*OV*) and that there was a 64 [34, 87] % chance that a score picked at random from the ChABC group would have been a higher score than a score picked at random from the Sham group (*PS*) (Fig. 2D). However, the fact that the range of the CIs of these estimators extends above and below 50% suggests that both distributions are quite similar.

General ECM enzymatic-digestion assessment in the apical region of the GCL (Fig. 2H) was performed before (Fig. 2I) and after conditioning (Fig. 2J). Four days after ChABC infusion, WFA intensity decreased in the ChABC group (5.14 [3.88, 7.55]) when compared to the Sham group (70.33 [63.42, 76.04]) ($\Delta_{Sh\text{–}Ch}$ = 65.20 [57.86, 71.11], $p = 5.91E{-}74$; Fig. 2E and F, II). Similar results were observed after the Acq test (Fig. 2J). ECM analysis yielded lower WFA intensity for the ChABC group (17.08 [14.66, 19.26]) than in the Sham group (79.18 [73.38,

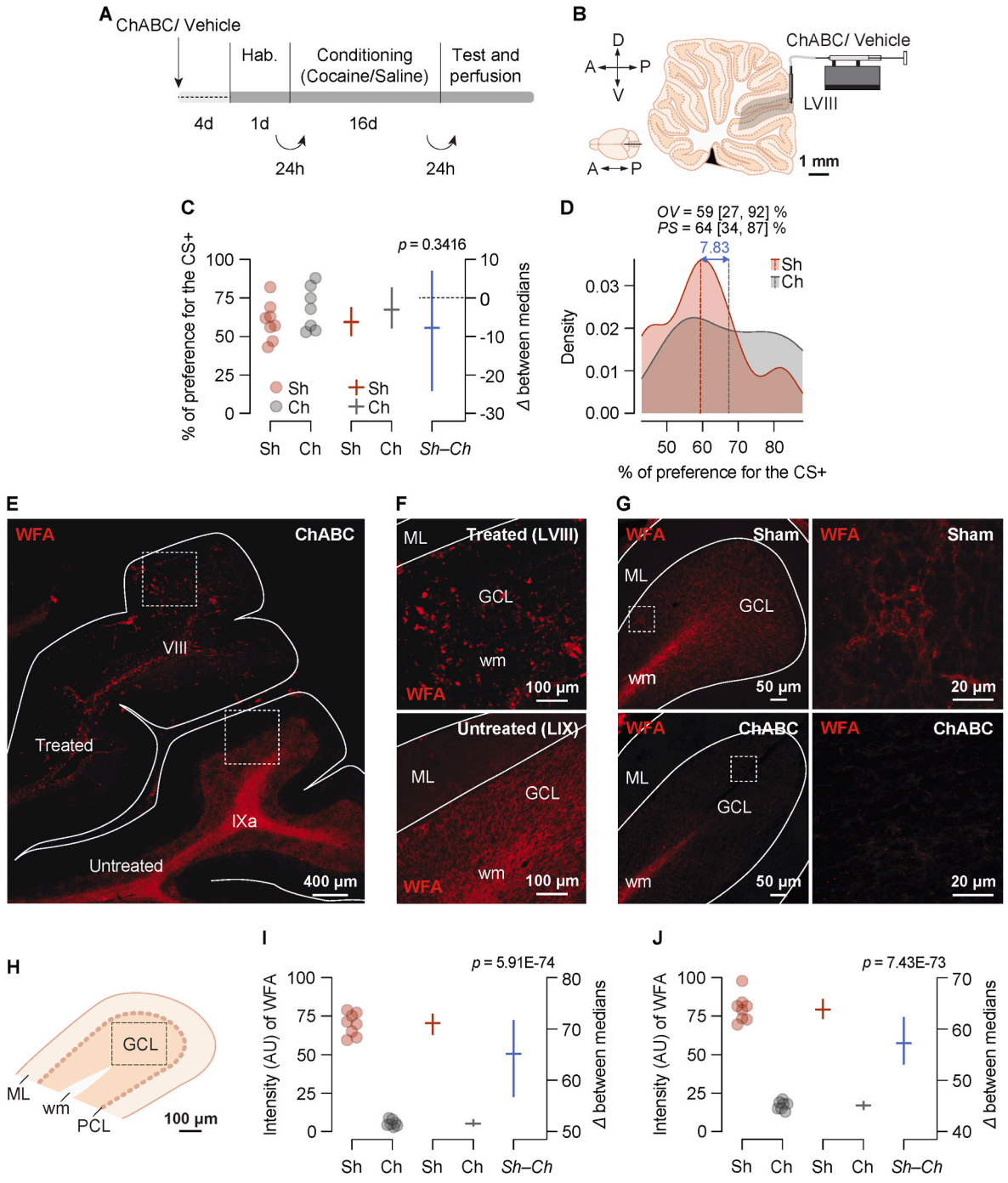

Fig. 2. Enzymatic digestion of PNNs in lobule VIII of the vermis does not affect acquisition of cocaine-induced preference conditioning. (A) Experiment timeline. **(B)** Schematic diagram of a sagittal section of the vermis depicting the injection site in lobule VIII (LVIII). **(C)** Behavioral effects of the infusion of ChABC (Ch, gray dots) or Vehicle (Sh, red dots) on cocaine-induced preference conditioning. **(D)** Sham and ChABC kernel density estimation of the % of preference for the CS + distributions with overlap (*OV*) and probability of superiority (*PS*) estimations and their 95% confidence intervals (95%CI) between both distributions. Dashed lines represent the median of each distribution, and the blue arrow represents the difference between them. **(E)** A representative confocal image (4 × 6 tile scan, 20x with a zoom of 2, and 2362 × 2362 px) of *Wisteria floribunda agglutinin* (WFA) staining in an animal 4 days after ChABC infusion in lobule VIII. Lobule IX was unaffected and works as a control for by ChABC-induced PNN digestion. **(F)** Representative magnifications of lobules VIII (LVIII; treated) and IX (untreated). ML: molecular layer; GCL: granule cell layer; wm: white matter. **(G)** Representative maximal projections of confocal images (3 × 3 tile scan, 25-step z-stack, 20x objective with a zoom of 2, and 2048 × 2048 px) of WFA staining in LVIII for the Sham (top panels) and the ChABC (bottom panels) groups after the preference test (23 days after ChABC infusion). Dashed squares represent the magnified regions in the images on the right (25-step z-stack maximal projections, 63x objective with a zoom of 2, and 2048 × 2048 px). Sham group magnification showing a PNN. **(H)** Schematics of a sagittal section of the different layers of the cerebellar cortex in LVIII. ML, molecular layer. WM, white matter. PCL, Purkinje cell layer. GCL, granule cells layer. Dashed line represents the area of the GCL where WFA intensity was assessed. General extracellular matrix WFA intensity assessment 4 days **(I)** and 22 days (after the Acq test) **(J)** following ChABC infusion. **(C, I, J)** Left to right. On the left axis: dot plot with jitter to avoid overlap between the points (semitransparent dots; each dot represents the score of each animal), and median (horizontal lines) plot with 95% CI (vertical lines). On the right axis we present the effect size as the difference between medians (Δ; horizontal line) and its 95% CI (vertical line). Sham ($n = 8$); ChABC ($n = 7$).

85.74]) ($\Delta_{Sh–Ch}$ = 62.10 [55.97, 68.69], p = 7.43E–73; Fig. 2G, J). No PNN was found either before or after conditioning training. Therefore, the acquisition of preference for cocaine-related cues was not affected despite WFA immunolabeling confirmed that ChABC effectively removed PNN expression in LVIII (Fig. 2E and F).

3.2. PNN digestion in lobule VIII disrupted cocaine-induced short-term memory

Following the Acq test, animals were randomly divided into Sham and ChABC groups for intra cerebellar infusions (Fig. 3). On the Acq test, both Sham (58.02 [54.47, 63.00]; n = 10) and ChABC (57.37 [50.54, 66.95]; n = 10) groups exhibited similar preference scores ($\Delta_{Sh–Ch}$ [95% CI] = 0.66 [–9.84, 9.84], p = 0.8840; Fig. 3C) and distributions ($OV_{Sh–Ch}$ = 45 [19, 70] %; $PS_{Sh–Ch}$ = 47 [23, 73] %; Fig. S1A). Thus, the acquisition test results in two equal distributions of 10 animals. Then, we infused ChABC/vehicle in LVIII (Fig. 3A and B) and performed another preference test to evaluate the short-term retention of memory (Ret). In this second test, the Sham group (58.02 [54.47, 63.00]) showed a higher preference score than the ChABC (48.02 group [43.23, 56.80]) ($\Delta_{Sh–Ch}$ [95% CI] = 26.30 [17.81, 36.49], p = 6.00E–8; Fig. 3C). Moreover, when comparing both distributions, we found minimum overlap ($OV_{Sh–Ch}$ = 13 [2, 24] %; Fig. 3D) between their kernel density estimations, and a low probability that a random score selected from the ChABC group is higher than a randomly selected one from the Sham group ($PS_{Sh–Ch}$ = 0 [0, 26] %; Fig. 3D). These two estimates and the KDEs of both groups allow us to confirm that both groups are different after PNN removal in LVIII.

The Sham group increased its preference score on the Ret test ($\Delta_{Acq–Ret}$ [95% CI] = −16.30 [–21.31, −11.57], p = 1.85E–6; Fig. 3C). Moreover, an analysis of the preference score distributions over tests revealed a small amount of overlap in the Sham group ($OV_{Acq–Ret}$ = 13 [2, 24] %; Fig. 3D) and showed a high probability of preference scores in the Ret test to be greater than those of the first test ($PS_{Acq–Ret}$ = 91 [65, 98] %; Fig. 3D). Looking at the KDE, we can also visually see a clockwise shift of the median scores in the Acq test regarding to the Ret test in the Sham group, indicating an increase in preference scores (Fig. 3D). Conversely, when comparing the preference scores of the ChABC group throughout tests (Acq vs Ret), we observed a decrease in preference in the Ret test ($\Delta_{Acq–Ret}$ [95% CI] = 9.34 [4.02, 17.08], p = 0.0051; Fig. 3C). The analysis of the distributions in the two tests showed a 55 [28, 82] % of overlap (Fig. 3D) and a lower probability of the scores in the Ret test to be greater than those of the first test ($PS_{Acq–Ret}$ = 23 [8, 49] %; Fig. 3D), thus revealing a reduction in preference (Fig. 3D).

To further understand the difference between Sham and ChABC groups, we quantified the proportion of change between both tests (slopegraph in Fig. 3C). In the Sham group, we observed that 0 [0, 4] % (p = 2.46E–125) of the animals decreased their preference score (100% of the animals increased their scores in the Ret test) while 90 [82, 95] % (p = 4.21E–69) of the animals treated with ChABC decreased their preference for the CS+ in the Ret test. When we calculated the proportion of change between both groups, we observed a difference of −90 [–96, −84] % ($\Delta_{Sh–Ch}$) between them (χ^2 = 163.64, p = 1.82E–37), revealing a changed in opposite directions.

Histological analyses confirmed that PNN digestion after the Acq test effectively reduced WFA expression in LVIII in 4 days (Fig. 3E). General ECM enzymatic-digestion assessment in the apical region of the GCL (Fig. 3F) showed a reduction of WFA intensity in the ChABC group (*Mdn* [95% CI] = 6.91 [5.80, 7.29]) when compared to the Sham group (*Mdn* [95% CI] = 63.23 [61.27, 69.06]) ($\Delta_{Sh–Ch}$ [95% CI] = 59.32 [54.56, 62.59], p = 3.02E–161; Fig. 3E, G). No PNNs in LVIII were found after ChABC infusion.

Our results showed that enzymatic digestion with ChABC in LVIII was not only able to prevent **incubation** of conditioned preference but also to disrupt short-term conditioned memory. Therefore, our findings suggest that intact PNNs around Golgi interneurons of the posterior vermis are needed to maintain short-term cocaine-induced Pavlovian associations.

3.3. PNN digestion in the DCN did not affect cocaine-induced short-term memory

In the present experiment, we wanted to test whether the digestion of PNNs in the DCN would affect short-term retention of cocaine-induced memory (Fig. 4). As we did in the previous experiment, animals were randomly divided into Sham and ChABC groups after the Acq test. On this test, both groups showed very similar preference scores ($\Delta_{Sh–Ch}$ [95% CI] = −1.30 [–17.67, 9.82], p = 0.8056; Fig. 4C) and distributions ($OV_{Sh–Ch}$ = 61 [34, 88] %; $PS_{Sh–Ch}$ = 56 [30, 78] %; Fig. S1B), (Sham (60.90 [44.89, 70.05]; n = 10) and ChABC (67.47 [55.05, 72.31]; n = 10)). Then, we infused ChABC in the DCN (Fig. 4A and B) and performed the Ret test. In this second preference test, the Sham group (62.21 [55.90, 70.43]) showed a similar preference score ($\Delta_{Sh–Ch}$ [95% CI] = 4.12 [–9.01, 14.89], p = 0.5156; Fig. 4C) to that of the ChABC group (60.35 [53.18, 70.04]). Moreover, the distributions of both groups were analogous ($OV_{Sh–Ch}$ = 66 [34, 98] %; $PS_{Sh–Ch}$ = 45 [22, 70] %; Fig. 4D). Then, we compared preference scores of each group over the Acq and Ret tests. For the Sham group, similar preference scores were observed for both tests ($\Delta_{Acq–Ret}$ [95% CI] = −3.57 [–14.87, 5.64], p = 0.3460; Fig. 4C) resulting in very close distributions ($OV_{Sh–Ch}$ = 71 [42, 100] %; $PS_{Sh–Ch}$ = 59 [33, 81] %; Fig. 4D). Similarly, comparable preference scores were observed for both tests in the ChABC group ($\Delta_{Acq–Ret}$ [95% CI] = 1.86 [–2.98, 9.02], p = 0.5588; Fig. 4C), generating alike distributions ($OV_{Sh–Ch}$ = 76 [47, 100] %; $PS_{Sh–Ch}$ = 44 [22, 69] %; Fig. 4D).

Next, we quantified the proportion of change between both tests (slopegraph in Fig. 4C). We observed that 20 [13, 29] % (p = 1.12E–09) of the animals in the Sham group and 57 [47, 67] % (p = 0.1933) of the animals in the ChABC group decreased their preference for the CS+ in the second test. When we compare the proportion of change of both groups, we observed a difference of −37 [–50, −25] % ($\Delta_{Sh–Ch}$) between them (χ^2 = 29.11, p = 6.84E–8), revealing greater proportion of change in the ChABC group.

Histological analyses confirmed that ChABC reduced WFA expression in DCN (Fig. 4E). General ECM enzymatic-digestion assessment (Fig. 4F) showed a reduction of WFA intensity in the ChABC group (*Mdn* [95% CI] = 13.84 [12.58, 16.04]) when compared to the Sham group (*Mdn* [95% CI] = 75.59 [68.54, 82.27]) ($\Delta_{Sh–Ch}$ [95% CI] = 61.75 [54.11, 68.28], p = 4.39E–10; Fig. 4E, G). Interestingly, we were able to find several weak PNNs after ChABC infusion in the DCN. Nevertheless, WFA intensity assessment yielded complementary results to those obtained for the ECM assessment. PNNs in the ChABC group (*Mdn* [95% CI] = 34.78 [32.81, 37.51]) exhibited reduced WFA intensity ($\Delta_{Sh–Ch}$ [95% CI] = 84.44 [56.93, 108.76], p = 9.11E–59; Fig. 4E, I) when compared to those in the Sham group (*Mdn* [95% CI] = 119.23 [90.48, 145.32]). As expected, we found a different frequency distribution of weak, medium, and strong PNNs between both groups ($\chi^2(2)$ = 206.72, p = 1.29E–45) (Fig. 4I and J). Post hoc analyses resulted in a larger proportion of weak PNNs in the ChABC group than in the Sham group ($\chi^2(1)$ = 206.64, p = 7.73E–47; $\Delta_{Sh–Ch}$ [95% CI] = −69 [–76, −76] %), while the proportion of medium ($\chi^2(1)$ = 133.79, p = 6.08E–31; $\Delta_{Sh–Ch}$ [95% CI] = 52 [44, 59] %) and strong ($\chi^2(1)$ = 38.36, p = 5.89E–10; $\Delta_{Sh–Ch}$ [95% CI] = 18 [12, 23] %) PNNs were greater in the Sham than in the ChABC group.

Our results suggest that PNNs in the DCN might not be necessary for

short-term maintenance of cocaine-induced conditioning. Nevertheless, although we did not observe any difference in the magnitude of preference between tests or groups, we observed a similar direction of change to that found under LVIII digestion.

3.4. Digestion of PNNs in lobule VIII facilitated extinction and reinstatement of cocaine-induced conditioned preference

To test the effects of an enzymatic digestion of PNNs in the cerebellar cortex on extinction (Fig. 5), rats were conditioned to cocaine and then, only animals that showed preference for the CS + underwent forced-extinction training (Fig. 1D) and reinstatement (Fig. 1E).

After conditioning, rats were randomly assigned to the ChABC or Sham groups. In the Acq test, rats from the ChABC (65.43 [64.05, 68.57]; $n = 6$) and Sham (67.24 [62.57, 73.35]; $n = 6$) groups exhibited similar preference scores (Δ_{Sh-Ch} [95% CI] = 1.81 [–3.85, 7.90], $p = 0.5696$; Fig. 5C) and distributions ($OV_{Sh-Ch} = 39$ [10, 67] %; $PS_{Sh-Ch} = 43$ [15, 76] %; Fig. S1C). Then, they received ChABC/vehicle in LVIII and 5 days later they underwent forced-extinction training.

On the first extinction test (Ext1) the ChABC (51.73 [44.35, 60.86])

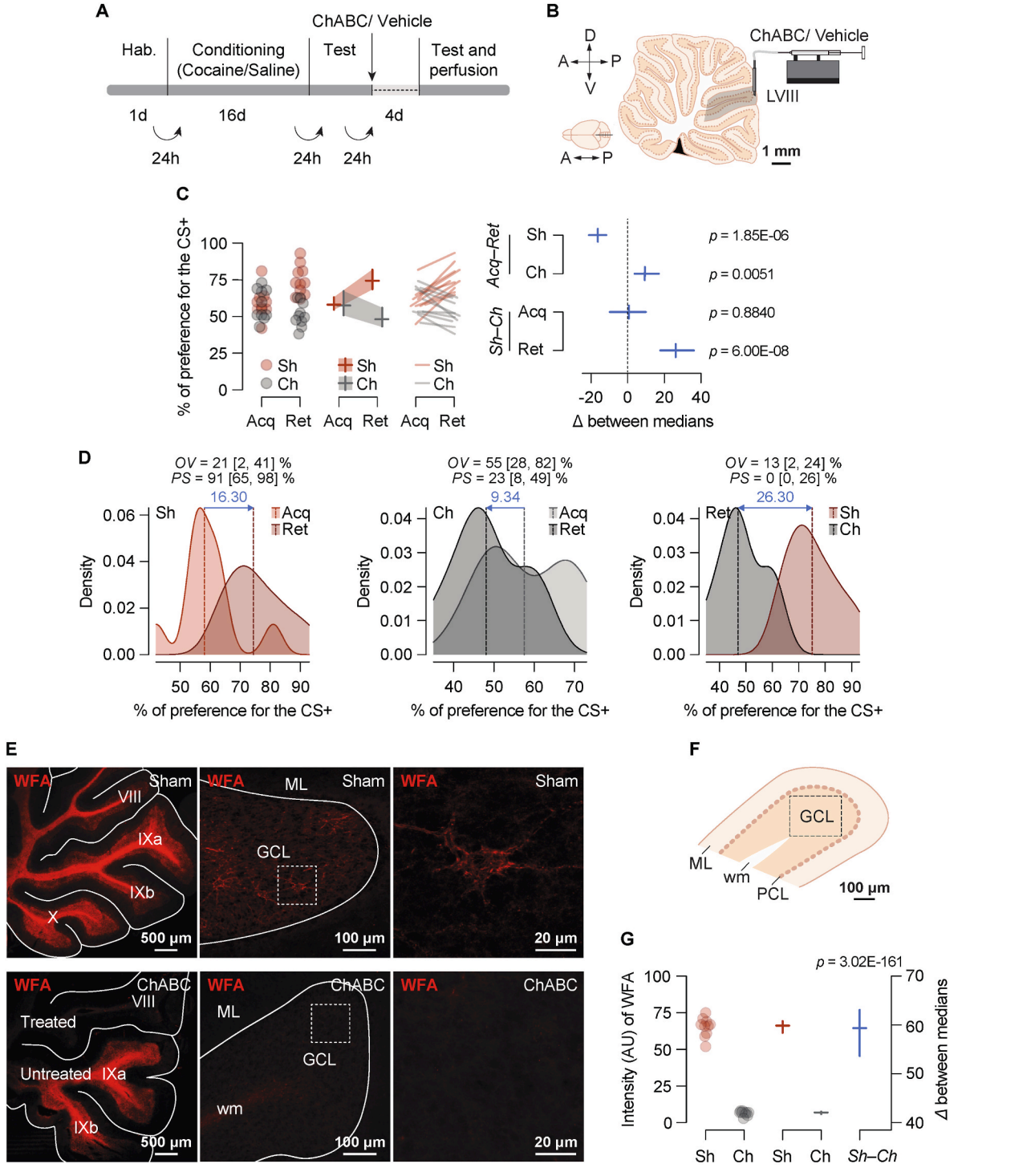

(caption on next page)

Fig. 3. Enzymatic digestion of PNNs in the posterior vermis after testing for preference disrupts cocaine-induced short-term memory. (A) Experiment timeline. **(B)** Diagram of a sagittal section illustrating the injection site in the posterior vermis, lobule VIII (LVIII). **(C)** Behavioral effects of ChABC infusion (Ch, gray) or Vehicle (Sh, red) on cocaine-induced preference conditioning. Left panel: 1) dot plot with jitter to avoid overlap between points (semitransparent dots; each dot represents the score of each animal); 2) jittered median plot with error bands, representing the medians (horizontal lines) with 95% confidence interval (95% CI; vertical lines and error bands); and 3) jittered slopegraph showing the direction of the change of each animal from the first (Acquisition, Acq) to the second (short-term memory, Ret) preference test (semitransparent lines). Right panel: we present the effect sizes (for the within-group and between-groups comparisons) as the difference between medians (*Δ*; vertical lines) and their 95% CI (horizontal lines). **(D)** Sham and ChABC kernel density estimation of the % of preference for the CS + distributions with overlap (*OV*) and probability of superiority (*PS*) estimations and their 95% CIs between both distributions. Left to right: Sh_{Acq} vs Sh_{Ret}, Ch_{Acq} vs Ch_{Ret}, and Ret_{Sh} vs Ret_{Ch}. Dashed lines represent the median of each distribution and blue arrow represents the shift of the median between Acq and Ret tests, and the difference between medians for the Sham and ChABC groups in the Ret test. **(E)** Representative confocal images of Wisteria floribunda agglutinin (WFA) staining 5 days after vehicle/ChABC infusion. Top and bottom panels represent the Sham and the ChABC groups respectively. From left to right: posterior cerebellum (5 × 5 tile scan, 20x with a zoom of 2, and 2362 × 2362 px), lobule VIII (LVIII) magnification (3× 3 tile scan, 25-step z-stack, 20x objective with a zoom of 2, and 2048 × 2048 px), dashed line magnification (25-step z-stack maximal projections, 63x objective with a zoom of 2, and 2048 × 2048 px). Sham group magnification shows a PNN. **(F)** Schematics of a sagittal section of the different layers of the cerebellar cortex in LVIII. ML, molecular layer. WM, white matter. PCL, Purkinje cell layer. GCL, granule cells layer. Dashed line represents the area of the GCL where WFA intensity was assessed. **(G)** General extracellular matrix WFA intensity assessment. Left to right. On the left axis: dot plot with jitter to avoid overlap between the points (semitransparent dots; each dot represents the score of each animal), and median (horizontal lines) plot with 95% CI (vertical lines). On the right axis we present the effect size as the difference between medians (*Δ*; horizontal line) and its 95% CI (vertical line). Sh: Sham ($n = 10$); Ch: ChABC ($n = 10$). Acq: preference test 24 h after cocaine-induced conditioning; Ret: preference test 5 days after ChABC infusion.

group showed a reduction of preference ($\Delta_{Sh–Ch}$ [95% CI] = 14.94 [1.52, 23.73], $p = 0.0116$; Fig. 5C) as compared to the Sham group (66.67 [55.76, 71.57]). This effect was also observed when comparing the KDEs of both groups. Although both distributions partially overlap 40 [3, 76] % ($OV_{Sh–Ch}$), there is only a 11 [2, 44] % ($PS_{Sh–Ch}$) chance that scores from the ChABC group are greater than those from the Sham group (Fig. 5D).

However, on the second extinction test (Ext2) both groups (Sham: 54.42 [44.30, 60.70]; ChABC: 49.11 [34.18, 66.33]) reached similar preference scores ($\Delta_{Sh–Ch}$ [95% CI] = 5.31 [–13.86, 21.07], $p = 0.5728$; Fig. 5C). Moreover, a third preference test conducted 8 days later (ExtLT) confirmed that both groups (Sham: 37.68 [24.96, 48.09]; ChABC: 44.50 [34.00, 55.21]) extinguished their preference for the CS+ ($\Delta_{Sh–Ch}$ [95% CI] = −6.81 [–22.00, 7.52], $p = 0.2924$; Fig. 5C). In fact, we observed a reduction in the preference score in the ExtLT test as compared to the Acq test in both the ChABC ($\Delta_{Acq–ExtLT}$ [95% CI] = 20.93 [8.84, 34.48], $p = 0.0017$; Fig. 5D, **S2B**) and Sham ($\Delta_{Acq–ExtLT}$ [95% CI] = 29.56 [18.72, 41.13], $p = 3.63E–07$; Fig. 5D, **S2A**) groups. Interestingly, after one reinstatement session in which a cocaine injection paired with the CS+, ChABC-treated rats reinstated (63.03 [55.46, 65.10]) whereas the Sham group did not (45.38 [34.55, 54.09]) ($\Delta_{Sh–Ch}$ [95% CI] = −17.66 [–28.76, −6.71], $p = 0.0017$; Fig. 5C). This can also be observed when comparing the distributions of both groups. Overlapping between the two distributions is low 14 [3, 33] % ($OV_{Sh–Ch}$) and there is a 94 [65, 99] % ($PS_{Sh–Ch}$) chance that scores from the ChABC group are greater than those from the Sham group (Fig. 5D), indicating that both distributions are quite different.

These results were supported by within comparisons in each group. While in the Sham group there was a decrease in preference scores from the Acq to the Reins test ($\Delta_{Acq–Reins}$ [95% CI] = 21.87 [16.69, 33.89], $p = 9.11E–07$; Fig. 5C, **S2A**), the ChABC group exhibited similar preference scores in both tests ($\Delta_{Acq–Reins}$ [95% CI] = 2.20 [–0.12, 6.77], $p = 0.2124$; Fig. 5C, **S2B**). Oppositely, the ChABC group increased their preference in the Reins test regarding the ExtLT ($\Delta_{ExtLT–Reins}$ [95% CI] = −18.54 [–30.57, −7.94], $p = 0.0017$; Fig. 5C, **S2B**) but the Sham group showed similar preference scores across both tests ($\Delta_{ExtLT–Reins}$ [95% CI] = −7.69 [–20.39, 3.16], $p = 0.3396$; Fig. 5C, **S2A**). Within-group distribution and sign test results can be found in **supplementary results**.

Histological analyses confirmed that ChABC before extinction reduced WFA expression in LVIII of the vermis (Fig. 5E). The cerebellar samples were taken 24 h after the Reins test and therefore, 25 days after the ChABC infusion. General ECM enzymatic-digestion assessment resulted in a reduction of WFA intensity in the ChABC group (24.28 [20.76, 26.98]) when compared to the Sham group (58.68 [48.87, 66.33]) ($\Delta_{Sh–Ch}$ [95% CI] = 34.40 [24.51, 41.95], $p = 6.18E–14$; Fig. 5F and G). Scattered PNNs were already found at that time, although WFA intensity assessment of these PNNs yielded similar results to those obtained for the ECM assessment. PNNs in the ChABC group (76.51 [55.89, 90.65]) showed reduced WFA intensity ($\Delta_{Sh–Ch}$ [95% CI] = 36.56 [13.53, 72.36], $p = 0.0028$; Fig. 5H and I) as compared to those in the Sham group (113.07 [93.29, 146.25]). Moreover, we found a different frequency distribution of weak, medium, and strong PNNs between both groups ($\chi^2(2)_{ShvsCh} = 23.75$, $p = 6.97E–06$, Fig. 5J). Post hoc analyses resulted in a larger proportion of weak PNNs in the ChABC group than in the Sham group ($\chi^2(1) = 23.17$, $p = 1.48E–06$; $\Delta_{Sh–Ch}$ [95% CI] = −43 [–59, −28] %). The proportion of medium PNNs were greater in the Sham than in the ChABC group ($\chi^2(1) = 16.21$, $p = 5.68E–05$; $\Delta_{Sh–Ch}$ [95% CI] = 37 [20, 53] %) and the proportion of strong PNNs was similar between both groups ($\chi^2(1) = 2.81$, $p = 0.0939$; $\Delta_{Sh–Ch}$ [95% CI] = 7 [–1, 14] %). These results suggest the existence of emerging PNNs around Golgi interneurons that were still maturating at the time of reinstatement.

Overall, these findings suggest that PNN in LVIII are not required for the formation of extinction, but for its maintenance. On the contrary, removal of these PNNs benefit the acquisition of extinction but also drug-induced reinstatement.

3.5. ECM and PNN expression correlate with preference for cocaine cues

To assess whether there is a relationship between the percentage of preference for cocaine-related cues (CS+) and the expression of ECM and PNN, we perfumed Spearman's rank correlation coefficient (*rho*) (Fig. 6, S3). First, we pulled all the animals together with enzymatic digestion in LVIII and assessed whether there was a relationship between the % of preference for the CS+ and the intensity (AU) of WFA related to the ECM. We observed a positive relationship between the two variables for both the Sham ($rho(22) = 0.62$ [0.28, 0.88], $p = 0.0013$) and the ChABC ($rho(21) = 0.71$ [0.45, 0.88], $p = 0.0002$) groups (Fig. 6A). Moreover, this relationship was maintained for both groups when correlating both variables individually for the Acq test (Sham: $rho(6) = 1.00$ [0.99, 1.00], $p = 4.96E–05$; ChABC: $rho(5) = 0.93$ [0.58, 0.99] $p = 0.0026$; Fig. S3A), and the Reins test (Sham: $rho(4) = 0.90$ [0.32, 0.99], $p = 0.0149$; ChABC: $rho(4) = 0.94$ [0.52, 1.00], $p = 0.0167$; Fig. S3D). However, this relationship was lost in the ChABC group in the Ret test, either with enzymatic digestion in LVIII (Sham: $rho(8) = 0.91$ [0.64, 0.99], $p = 0.0002$; ChABC: $rho(8) = 0.30$ [–0.41, 0.78], $p = 0.3983$; Fig. S3B) or in the DCN (Sham: $rho(8) = 0.90$ [0.53, 1.00], $p = 0.0004$; ChABC: $rho(8) = 0.56$ [–0.24, 0.96], $p = 0.0935$; Fig. S3C).

We observed similar positive results regarding the relationship between the % of preference for the CS+ and the intensity (AU) of WFA in the PNNs (Fig. 6B and C). A positive relationship was observed for both groups in the Ret test with digestion in DCN (Sham: *rho*(8) = 0.92 [0.60, 1.00], p = 0.0002; ChABC: *rho*(8) = 0.71 [0.04, 0.94], p = 0.0218; Fig. 6B) and the Reins test with digestion in LVIII (Sham: *rho*(8) = 0.94 [0.50, 1.00], p = 0.0167; ChABC: *rho*(8) = 0.94 [0.56, 0.99], p = 0.0048; Fig. 6C).

Our results show that both cerebellar ECM and PNN expression seems to be highly related to the degree of the preference displayed toward cocaine cues. Interestingly, this effect is lost for loose ECM 5 days after enzymatic digestion with ChABC, but not for PNNs.

4. Discussion

Perineuronal net functions are still under investigation, but they

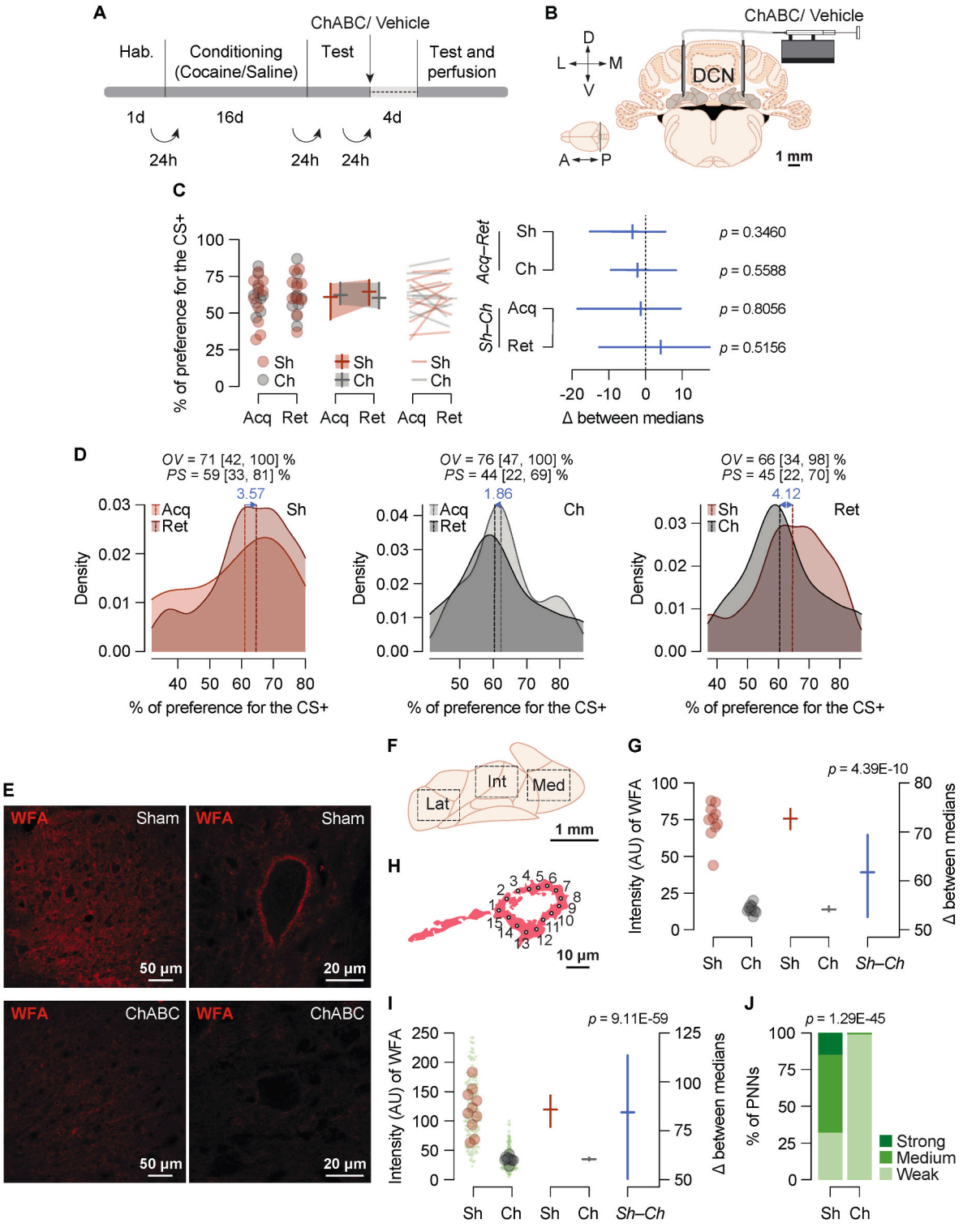

(caption on next page)

Fig. 4. Enzymatic digestion of PNNs in the DCN after testing for preference does not affect cocaine-induced short-term memory. (A) Experiment timeline. **(B)** Schematic diagram depicting the injection site in the deep cerebellar nuclei (DCN). **(C)** Behavioral effects of the infusion of ChABC or Vehicle on cocaine-induced preference conditioning for the Sham (Sh, red) and ChABC (Ch, gray) groups. Left panel: 1) dot plot with jitter to avoid overlap between the points showing each score (semitransparent dots; each dot represents the score of each animal); 2) jittered median plot with error bands, representing the medians (horizontal lines) with 95% confidence interval (95% CI; vertical lines and error bands); and 3) jittered slopegraph showing the direction of the change of each animal from the fist to the second preference test (semitransparent lines). Right panel: we present the effect sizes (for the within-group and between-groups comparisons) as the difference between medians (*Δ*; vertical lines) and their 95% CI (horizontal lines). **(D)** Sham and ChABC kernel density estimation of the % of preference for the CS + distributions with overlap (*OV*) and probability of superiority (*PS*) estimations and their 95% CIs between both distributions. Left to right: Sh_{Acq} vs Sh_{Ret}, Ch_{Acq} vs Ch_{Ret}, and Ret_{Sh} vs Ret_{Ch}. Dashed lines represent the median of each distribution and blue arrow represents the shift of the median (between the Acq and the Ret test) or the difference between medians (Sham vs ChABC group in the Ret test). **(E)** Left panels show representative confocal images (3 × 3 tile scan, 25-step z-stack, 20x objective with a zoom of 2, and 2048 × 2048 px) of WFA staining in two animals with Sham or ChABC infusions in the DCN. Right panels show representative confocal images (25-step z-stack maximal projections, 63x objective with a zoom of 2, and 2048 × 2048 px) of PNNs in the DCN. **(F)** Diagram depicting the DCN. Dashed lines delineate the areas where WFA intensity was assessed. **(G)** General ECM WFA intensity assessment after the Ret test for the Sham and the ChABC groups. **(H)** PNN intensity assessment was done as arbitrary units (AU) of WFA by averaging 15 randomly-placed points around the somatic region of the PNN. **(I)** PNN intensity assessment after the Ret test. Small green dots represent each single PNN (20 per animal, 200 per group). **(G, I)** On the left axis: dot plot with jitter to avoid overlap between the points (semitransparent dots; each dot represents the score of each animal), and median (horizontal lines) plot with 95% CI (vertical lines). On the right axis we present the effect size as the difference between medians (*Δ*; horizontal line) and its 95% CI (vertical line). **(J)** Proportion of weak (0–85 AU of intensity), medium (86–170 AU of intensity) and strong (171–255 AU of intensity) PNNs in the Sham and ChABC groups. Data is shown using stacked bars. Sh: Sham ($n = 10$); Ch: ChABC ($n = 10$). Acq: preference test 24 h after cocaine-induced conditioning; Ret: preference test 5 days after ChABC infusion.

involved ion-buffering (Brückner et al., 1993), protection against oxidative stress (Cabungcal et al., 2013; Morawski et al., 2004), and synaptic plasticity (Faissner et al., 2010; Wang and Fawcett, 2012). Perineuronal nets have been proposed as key mechanisms through which drug-induced long-lasting memories could be maintained (Carbo-Gas et al., 2017; Lasek et al., 2018; Slaker et al., 2016; Van Den Oever et al., 2010). It has been suggested that strong PNNs could "stamp in" synaptic connections that represent drug-cue associative memory and hamper future synaptic remodeling (Sorg et al., 2016).

In the present research, we investigated the role of cerebellar PNNs on acquisition, retention, extinction, and reinstatement of cocaine-induced conditioned preference. We infused the enzyme ChABC into the posterior vermis and DCN to digest PNNs around Golgi interneurons and output neurons of the cerebellum, respectively. ChABC effectively degraded CSPGs and disrupted PNNs in both cerebellar regions as previously shown (Carulli et al., 2020; Corvetti and Rossi, 2005). The degradation of PNNs around Golgi cells was evident 4 days after ChABC infusion and lasted for 3 weeks (Fig. 7). All experiments were conducted within this temporal window. In the DCN, ChABC also disrupted PNNs, although in some animals we found faint emerging PNNs scattered.

Our findings indicate that enzymatic digestion of PNNs around Golgi cells in the posterior vermis did not affect cocaine-induced Pavlovian learning. However, disruption of these PNNs after testing blocked the preference response. After acquisition, conditioned preference increased over time in the Sham group but decreased when PNNs were disrupted. The incubation of conditioned preference after repeated tests has been previously described for cocaine (Sakoori and Murphy, 2005). Nevertheless, the role of PNNs in the incubation of preference is still unknown. Recently, it has been shown that the incubation of a nociceptive effect involves PNN upregulation in the somatosensory cortex (Mascio et al., 2022).

The present investigation also reveals that the formation of extinction memory was facilitated after PNN digestion in the posterior vermis. Paradoxically, although extinction appeared to be facilitated under PNNs degradation, ChABC- but not sham-reated rats reinstated after receiving a priming injection of cocaine. A detailed examination of the extinction curve over time showed no differences between the sham and ChABC groups after 6 extinction trials (the second extinction test).

Our findings suggest a role for cerebellar PNNs in short-term memory of cocaine-induced conditioned memory. Removal of PNNs could prevent the stabilization of cocaine-induced memory and undermined its retention. It is also possible that removal of PNN disrupted reconsolidation of cocaine-induced memory. However, if it were the case, reinstatement of cocaine-induced memory would be prevented after extinction, as it happens in the PL (Slaker et al., 2015), but we found the opposite result.

Alternatively, removal of PNNs could favor cocaine-induced memory update during the second test and given that the preference test worked as an extinction trial the update would benefit extinction and decrease preference. Still, the crucial point is why PNN disruption after testing was able to encourage reinstatement of cocaine-induced memory 3 weeks later. Our hypothesis is that PNNs in the cerebellar cortex are required for both stabilization of drug-induced conditioned memory and the maintenance of extinction. Removal of PNNs did not eliminate cocaine-induced memory but originated instability in the memory trace that could accelerate the formation of extinction memory, since both kinds of memory partially compete each other (Dunsmoor et al., 2015). We speculate that if the newly formed extinction memory consolidated the original drug-induced memory would not reappear after 3 weeks. Therefore, our hypothesis is that extinction memory could not be stabilized without PNNs, and the new cocaine injection was sufficient to reinstate cocaine-induced memory. We cannot rule out, however, that PNN degradation boosted acute cocaine effects during reinstatement. In fact, one of the functions of PNNs is to protect fast spiking neurons against oxidative stress (Sorg et al., 2016). It is known that cocaine alters the redox status and increases the accumulation of reactive oxidative species (Womersley et al., 2019). Moreover, dynamic regulation of PNN structure depends on metalloproteinases (MMPs) (Ferrer-Ferrer and Dityatev, 2018). Given that at the time point of reinstatement we showed a partial restoration of PNNs around Golgi cells, one would expect an increase in metalloproteinase activity that could have boosted cocaine effects. In support, MMP inhibition reduces preference for cocaine (Brown et al., 2017).

In contrast to the cerebellar cortex, digestion of PNNs around the output neurons in the DCN did not affect cocaine-induced conditioned preference. Accordingly, our previous correlational findings indicated that only PNNs surrounding Golgi interneurons appear to play a role in drug-related memory (Carbo-Gas et al., 2017). Golgi-bearing PNNs in the apical region of the cerebellar vermis increased exclusively when animals expressed cocaine-induced conditioned preference. In contrast, PNN expression in the DCN decreased in all cocaine-treated groups regardless of they received cocaine either contingently or randomly (Carbo-Gas et al., 2017).

A source of discrepancy in the present investigation arises when comparing results between the sham groups in the experiments 2 and 3. While cocaine-induced conditioned preference incubated in the sham

group in experiment 2 (Fig. 3C and D) (lobule VIII), this effect was not replicated for sham-treated rats when the cannula was in the DCN in the experiment 3 (Fig. 4C and D). Nevertheless, a detailed analysis of the Acq (test 1) versus Ret (test 2) distributions in this experiment reveals a similar trend toward increasing conditioned preference in the Ret test. There is no a clear explanation for this discrepancy, but the more ventral location and trajectory of the cannula in the DCN could be relevant factors.

The present findings do not mimic ChABC effects in the PL or the anterior dorsal hypothalamic area (Blacktop et al., 2017; Slaker et al., 2015). PNN removal around PV + GABAergic interneurons in these areas prevented acquisition (Blacktop et al., 2017; Slaker et al., 2015), reinstatement (Slaker et al., 2015), and reconsolidation of CPP in rats (Slaker et al., 2015). Moreover, in contrast to the cerebellum, depletion of PNNs in the amygdala abolished priming-induced reinstatement of cocaine- and morphine-induced CPP when ChABC was combined with extinction training (Xue et al., 2014).

Our research is the first study that explores the role of PNNs around Golgi interneurons in drug-induced learning and memory. An earlier study investigated the role of PNNs in the DCN in eye blink conditioning, a form of Pavlovian motor learning (Carulli et al., 2020). Contrary to our results, enzymatic digestion of PNNs in the DCN improved eye blink conditioning but disrupted retention of the motor memory that declined over time.

Altogether, evidence suggests that the effects of PNN disruption on drug-related memory rely on the functional specialization of the circuits

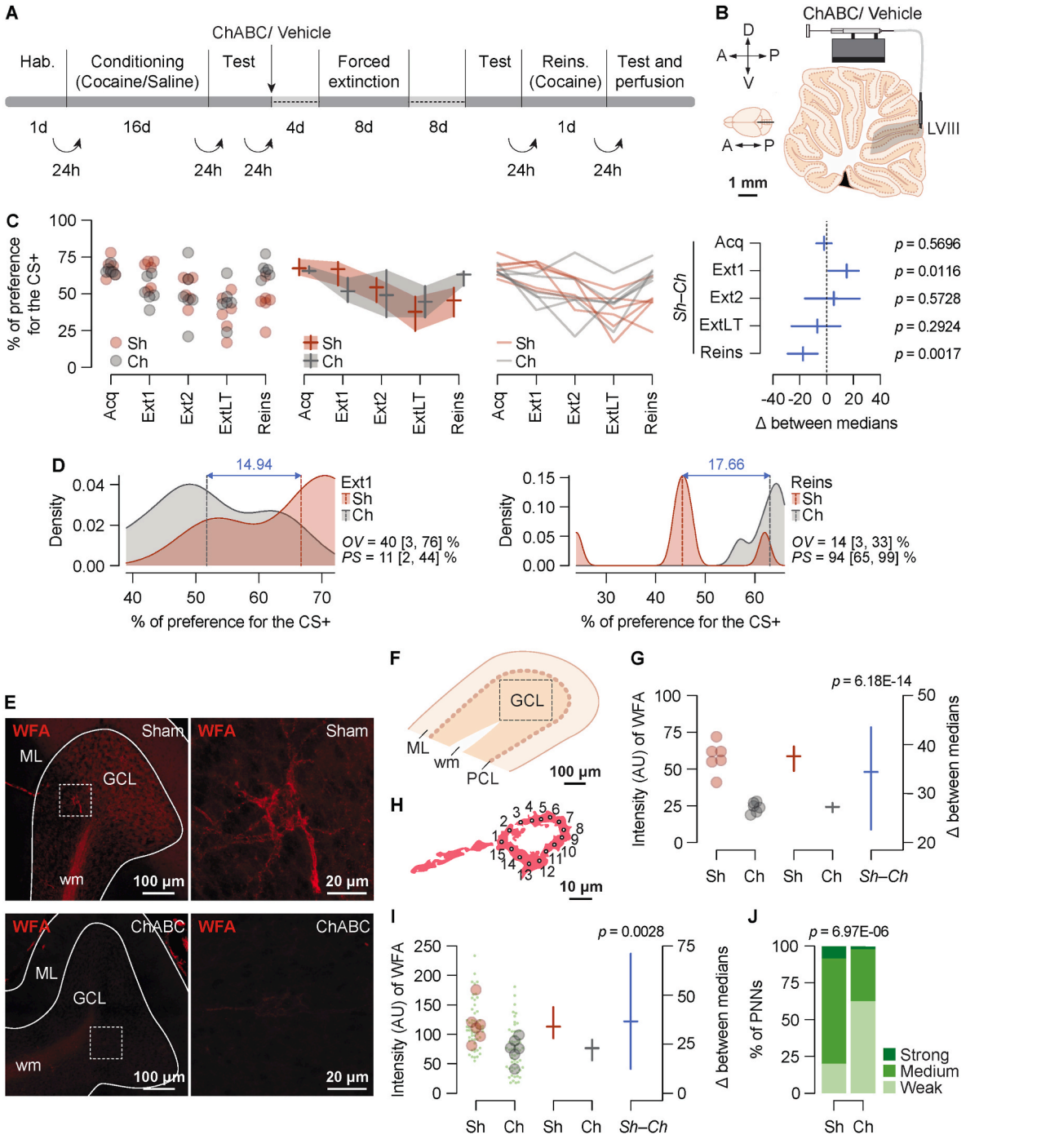

(caption on next page)

Fig. 5. Enzymatic degradation of PNNs in lobule VIII facilitates the formation of extinction memory but also encourages reinstatement of cocaine-induced preference memory. (A) Experiment timeline. **(B)** Diagram of a sagittal section illustrating the injection site in lobule VIII. **(C)** Behavioral effects of the infusion of ChABC or Vehicle on cocaine-induced preference conditioning for the Sham (red) and ChABC (gray) groups. Left panels: 1) dot plot with jitter to avoid overlap between the points showing each score (semitransparent dots; each dot represents the score of each animal); 2) jittered median plot with error bands, representing the medians (horizontal lines) with 95% confidence interval (95% CI; vertical lines and error bands); and 3) jittered slopegraph showing the direction of the change in each animal from the first to the second preference test (semitransparent lines). Right and bottom panels represent the effect sizes (for the within-group and between-groups comparisons) as the difference between medians (*Δ*; vertical lines) and their 95% CI (horizontal lines). **(D)** Sham and ChABC kernel density estimation of the % of preference for the CS + distributions, and overlap (*OV*) and probability of superiority (*PS*) estimations with their 95% CIs between both distributions. Left to right: $Ext1_{Sh}$ vs $Ext1_{Ch}$ and $Reins_{Sh}$ vs $Reins_{Ch}$. Dashed lines represent the median of each distribution and blue arrow represents the difference between medians (Sham vs ChABC group in the first extinction test and the reinstatement test; Ext1 and Reins respectively). **(E)** Left panels show representative confocal images (3 × 3 tile scan, 25-step z-stack, 20x objective with a zoom of 2, and 2048 × 2048 px) of Wisteria floribunda agglutinin (WFA) staining in an animal with Sham and ChABC infusion in LVIII. Right panels show a magnification of the white dotted squares on the left images (25-step z-stack maximal projections, 63x objective with a zoom of 2, and 2048 × 2048 px) of PNNs in LVIII. **(F)** Schematics of a sagittal section of the different layers of the cerebellar cortex in LVIII. ML, molecular layer. WM, white matter. PCL, Purkinje cell layer. GCL, granule cells layer. Dashed line represents the area of the GCL where WFA intensity was assessed. **(G)** General ECM WFA intensity assessment after the reinstatement (Reins) test for the Sham and the ChABC groups. **(H)** PNN intensity is shown as arbitrary units (AU) of WFA by averaging 15 randomly-placed points around the somatic region of the PNN. **(I)** PNNs intensity assessment after Reins test. Small green dots represent each single PNN (10 per animal, 60 per group). **(G, I)** Left to right. On the left axis: dot plot with jitter to avoid overlap between the points (semitransparent dots; each dot represents the score of each animal), and median (horizontal lines) plot with 95% confidence interval (95% CI; vertical lines). On the right axis we present the effect size as the difference between medians (*Δ*; horizontal line) and its 95% CI (vertical line). **(J)** Weak (0–85 AU of intensity), medium (86–170 AU of intensity), and strong (171–255 AU of intensity) PNN frequency distribution in the Sham and ChABC groups. Data is shown using stacked bars. Sh: Sham ($n = 6$); Ch: ChABC ($n = 6$). Acq: test after cocaine-conditioning training; Ext1: first extinction test; Ext2: second extinction test; ExtLT: long-term extinction test; Reins: reinstatement test.

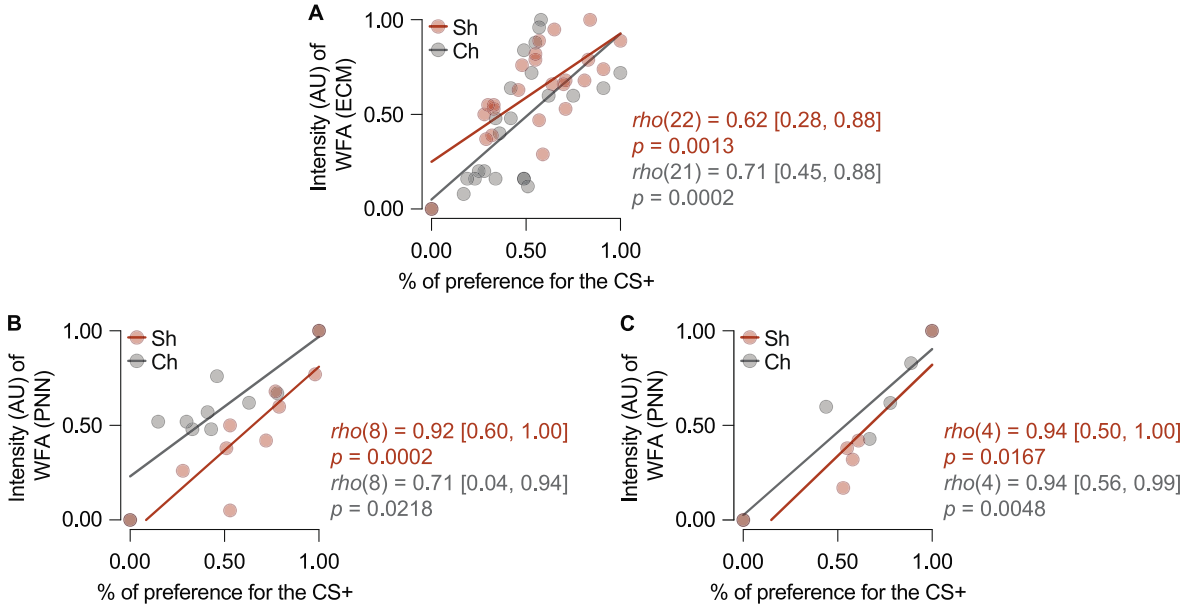

Fig. 6. Changes in preference for cocaine-related cues are correlated with changes in the expression of both ECM and PNNs. Scatterplots and Spearman's rank correlation coefficients (*rho*) with line of best fit between the % of preference for the CS+ and **(A)** LVIII ECM expression after Acq (test after cocaine-conditioning training), Ret (short-term retention test), and Reins (reinstatement test), **(B)** PNN expression in DCN after Ret, and **(C)** PNN expression in LVIII after Reins. Sh: Sham (**A**: $n = 24$; **B**: $n = 10$; **C**: $n = 6$); Ch: ChABC (**A**: $n = 23$; **B**: $n = 10$; **C**: $n = 6$).

to which PNN-expressing neurons belong (Carbo-Gas et al., 2017). The present findings suggest that encoding of drug-induced Pavlovian memory does not involve cerebellar mechanisms; otherwise, one could expect acquisition to be affected by PNN digestion, as described for the PL cortex (Slaker et al., 2015). PNNs around Golgi interneurons, however, seem to contribute to maintain cocaine-cue associations. Moreover, PNN digestion could undermine the stability of the original cocaine-olfactory cue engram and facilitate the formation of extinction memory. Nevertheless, since removal of PNNs around Golgi cells only destabilizes but not eliminates the original engram, it may be reactivated by the unconditioned stimulus (cocaine injection). Therefore, PNNs in the cerebellar cortex may act as mechanisms for stabilization of synaptic changes representing drug-cue engrams that were created in distal regions such as the amygdala, PL and infralimbic cortex. This information will be conveyed to the cerebellar cortex by mossy and climbing afferents from the pontine nuclei and inferior olive, respectively.

In the cerebellar cortex, Golgi interneurons are essential regulators of cerebellar plasticity and activity (Armano et al., 2000; D'Angelo et al., 2013, 1999). Their axons inhibit and synchronize activity in granule cells (Tabuchi et al., 2018). At the same time, Golgi cell activity is controlled by glutamatergic inputs from granule cells and mossy fibers (Palay and Chan-Palay, 1974), as well as by GABAergic and glycinergic inhibitory interneurons (Dumoulin et al., 2001; Sotelo and Llinás, 1972). Golgi cells act as a filter for the transmission of neural information from the granule cells and mossy fibers to Purkinje dendrites (D'Angelo et al., 2013; Galliano et al., 2010; Prestori et al., 2019). Importantly, we have shown that cocaine-induced conditioned memory is associated with

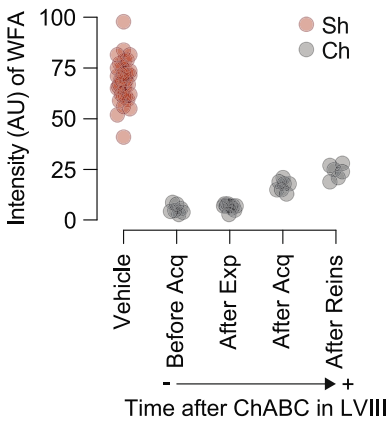

Fig. 7. Evolution of WFA recovery over time. Dot plot with jitter to avoid overlap between the points showing each score (semitransparent dots; each dot represents the score of each animal) showing the evolution of WFA expression after ChABC digestions in lobule VIII. Sh: Sham ($n = 32$); Ch: ChABC (Before Acq, $n = 7$; Before Ret, $n = 10$; After Acq, $n = 7$; After Reins $n = 6$). Acq: test after cocaine-conditioning training; Ret: short-term retention test; Reins: reinstatement test.

increased activity in granule cells and Golgi interneurons bearing strong PNNs (Carbo-Gas et al., 2014a, 2014b, 2017).

To our knowledge, no study has addressed the functional consequences of PNN removal around Golgi cells. Enzymatic digestion of PNNs around PV + neurons increase variability of spiking and instability of the firing patterns (Christensen et al., 2021; Miao et al., 2017). Brown and Sorg (2022) have speculated that natural dynamic remodeling of PNN could regulate low and high frequency firing patterns to optimize neural inputs. PNN alterations could degrade spatiotemporal neural representations of external information and alter synchronization across related brain regions.

5. Shortcomings

The bacterial enzyme ChABC not only digests the chondroitin sulfate glycosaminoglycans of the CSPG and the hyaluronan in the PNN but also in the loose ECM and white matter (Brückner et al., 1998; Fox and Caterson, 2002; Prabhakar et al., 2005). White matter in the cerebellar cortex comprises Purkinje descending GABAergic projections to the DCN and some glial cells. It has been described that ChABC is able to promote increased density and total length of Purkinje axons that picks after 7 days and lasts for 21 days after infusion (Corvetti and Rossi, 2005). In addition, these authors described that ChABC infusion does not disrupt the relationship between Purkinje axons and myelin sheaths, although myelinated Purkinje axon were surrounded by a dense meshwork of unmyelinated in the GCL of ChABC treated cerebella. Hence, we cannot rule out the contribution of loose ECM degradation and structural plasticity in Purkinje to the present behavioral effects.

The present research did not test the PNN's role in the expression of cocaine-induced conditioned memory but only in short-term memory after its expression. Thus, we do not know whether a prior expression of the conditioned response could contribute to the present effects. Neither we investigated sex differences in the expression of PNNs in the cerebellum. To our knowledge, no study has addressed this question. Only a few papers have explored sex differences in PNN expression (Ciccarelli et al., 2021; Gildawie et al., 2020; Guadagno et al., 2020), and no consistent differences have been found. Nevertheless, males tend to show a higher PNN expression in several brain regions with sexual dimorphism as the medial amygdala (Ciccarelli et al., 2021). Future research will clarify this issue for PNN expression in the cerebellum.

Funding

UJI-B2020-1 funded by Plan de promoción de la investigación (MM); (PND-132400) funded by Plan Nacional de Drogas 2017 (MM); PGC2018-095980-B-I00 funded by MCIN/AEI/10.13039/501100011033 and by "ERDF A way of making Europe" (MM); BES-2016-076353 funded by MCIN/AEI/10.13039/501100011033 and by "ESF investing in your future" (ASH); Grant ACIF/2019/109 funded by Conselleria d'Innovació, Universitats, Ciència i Societat Digital (PIM); Grant PRE2019-088521 funded by MCIN/AEI/10.13039/501100011033 and by "ESF investing in your future" (IME).

CRediT authorship contribution statement

Julian Guarque-Chabrera: Methodology, Formal analysis, Investigation, Writing – original draft, Writing – review & editing, Visualization. **Aitor Sanchez-Hernandez:** Investigation, Writing – review & editing. **Patricia Ibáñez-Marín:** Investigation, Writing – review & editing. **Ignasi Melchor-Eixea:** Investigation, Writing – review & editing. **Marta Miquel:** Conceptualization, Methodology, Formal analysis, Writing – original draft, Writing – review & editing, Funding acquisition, All authors approved the present version of the manuscript.

Declaration of competing interest

The authors declare that the research was conducted in the absence of any commercial or financial relationships that could be construed as a potential conflict of interest.

Data availability

Data base is included as a .xlsx file.

Acknowledgements

We are grateful to Dr. Carla Sanchis-Segura for her expert advice in statistics. We also thank SCIC (Servicio Central de Instrumentación Científica, Universitat Jaume I) for the assistance during confocal imaging acquisition.

Appendix A. Supplementary data

Supplementary data to this article can be found online at https://doi.org/10.1016/j.neuropharm.2022.109210.

Appendix A. Flowcharts I. (A.1) Effects of ChABC infusions in the cerebellar lobule VIII vermis before cocaine-induced preference conditioning. (A.2) Effects of ChABC infusions in the cerebellar lobule VIII vermis before short-term memory

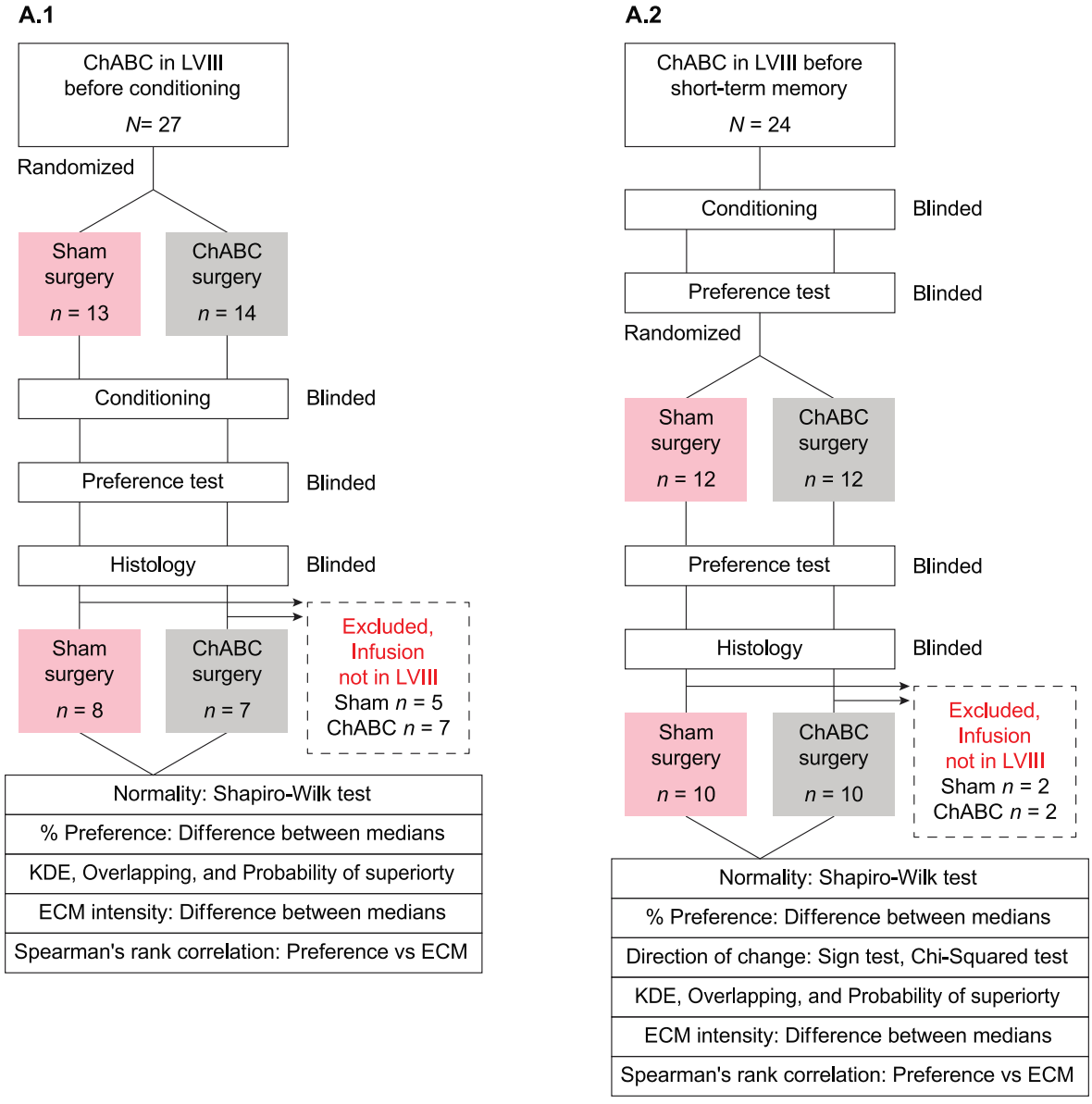

Appendix B. Flowcharts II. (B.1) Effects of ChABC infusions in the deep cerebellar nuclei before short-term memory. (B.2) Effects of ChABC infusions in cerebellar lobule VIII vermis before extinction and reinstatement

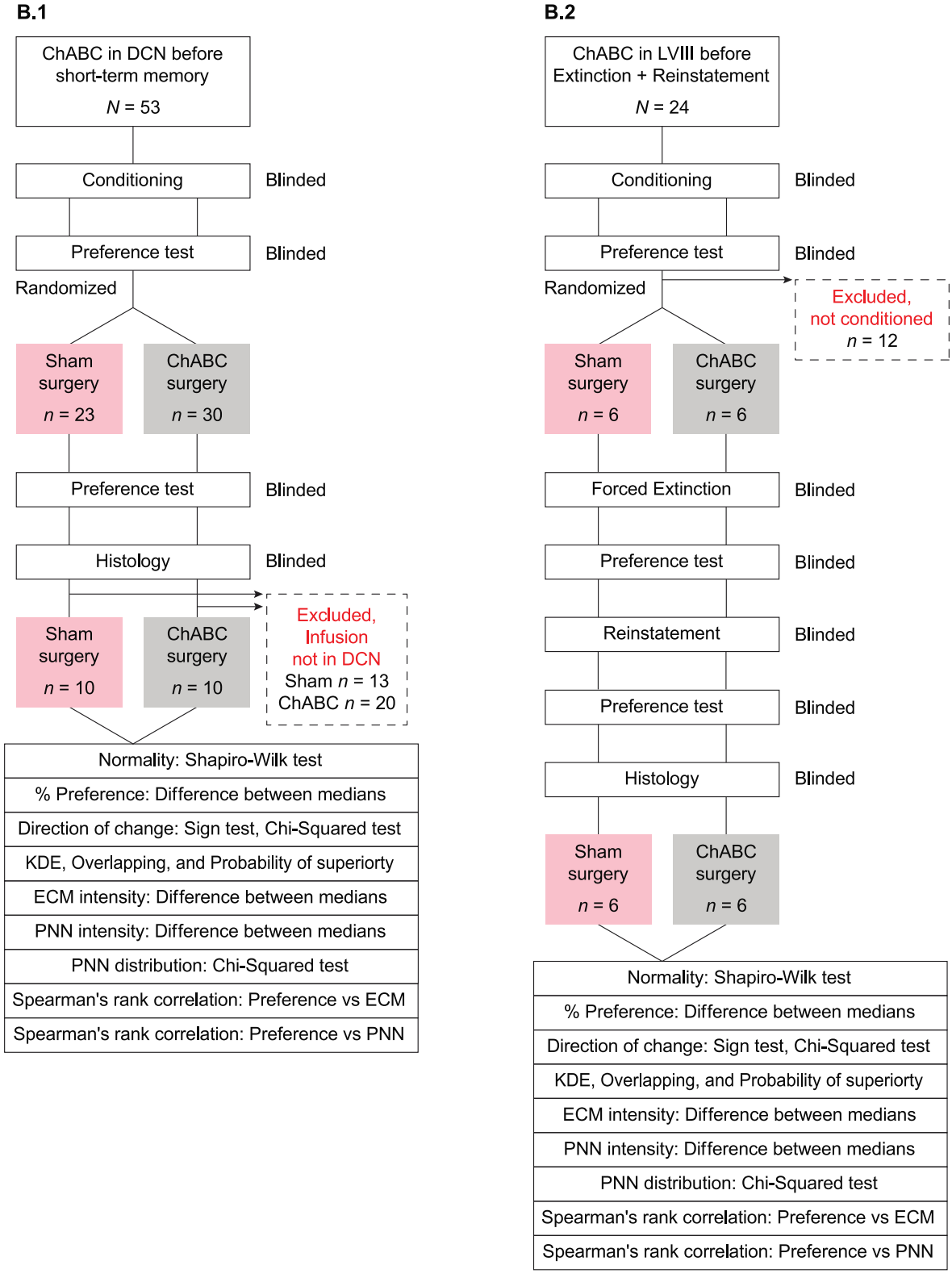

References

Altman, D., Machin, D., Bryant, T.N., Gardner, M.J., 2000. Statistics with confidence: confidence intervals and statistical guidelines. In: Records of the IEEE International Workshop on Memory Technology, Design and Testing, second ed. London, England.

Anderson, S.F., 2019. Misinterpreting p: the discrepancy between p values and the probability the null hypothesis is true, the influence of multiple testing, and implications for the replication crisis. Psychol. Methods 25, 596–609. https://doi.org/10.1037/met0000248.

Armano, S., Rossi, P., Taglietti, V., D'Angelo, E., 2000. Long-term potentiation of intrinsic excitability at the mossy fibergranule cell synapse of rat cerebellum. J. Neurosci. 20, 5208–5216. https://doi.org/10.1523/jneurosci.20-14-05208.2000.

Baguley, T., 2009. Standardized or simple effect size: what should be reported? Br. J. Psychol. 100, 603–617. https://doi.org/10.1348/000712608X377117.

Benjamini, Y., Hochberg, Y., 1995. Controlling the false discovery rate: a practical and powerful approach to multiple testing. J. R. Stat. Soc. Ser. B 57, 289–300. https://doi.org/10.1111/j.2517-6161.1995.tb02031.x.

Bernard, C., 2019. Changing the way we report, interpret, and discuss our results to rebuild trust in our research. eNeuro 6, 4–6. https://doi.org/10.1523/ENEURO.0259-19.2019.

Blacktop, J.M., Sorg, B.A., 2019. Perineuronal nets in the lateral hypothalamus area regulate cue-induced reinstatement of cocaine-seeking behavior. Neuropsychopharmacology 44, 850–858. https://doi.org/10.1038/s41386-018-0212-8.

Blacktop, J.M., Todd, R.P., Sorg, B.A., 2017. Role of perineuronal nets in the anterior dorsal lateral hypothalamic area in the acquisition of cocaine-induced conditioned place preference and self-administration. Neuropharmacology 118, 124–136. https://doi.org/10.1016/j.neuropharm.2017.03.018.

Bostan, A.C., Strick, P.L., 2018. The basal ganglia and the cerebellum: nodes in an integrated network. Nat. Rev. Neurosci. 19 (6), 338–350. https://doi.org/10.1038/s41583-018-0002-7.

Brown, T.E., Sorg, B.A., 2022. Net gain and loss: influence of natural rewards and drugs of abuse on perineuronal nets. Neuropsychopharmacology 1–18. https://doi.org/10.1038/s41386-022-01337-x.

Brückner, G., Brauer, K., Härtig, W., Wolff, J.R., Rickmann, M.J., Derouiche, A., Delpech, B., Girard, N., Oertel, W.H., Reichenbach, A., 1993. Perineuronal nets provide a polyanionic, glia-associated form of microenvironment around certain neurons in many parts of the rat brain. Glia 8, 183–200. https://doi.org/10.1002/glia.440080306.

Brückner, G., Bringmann, A., Härtig, W., Köppe, G., Delpech, B., Brauer, K., 1998. Acute and long-lasting changes in extracellular-matrix chondroitin-sulphate proteoglycans induced by injection of chondroitinase ABC in the adult rat brain. Exp. Brain Res. 121, 300–310. https://doi.org/10.1007/s002210050463.

Cabungcal, J.H., Steullet, P., Morishita, H., Kraftsik, R., Cuenod, M., Hensch, T.K., Do, K. Q., 2013. Perineuronal nets protect fast-spiking interneurons against oxidative stress. Proc. Natl. Acad. Sci. U.S.A. 110, 9130–9135. https://doi.org/10.1073/pnas.1300454110.

Calin-Jageman, R.J., 2018. The new statistics for neuroscience majors: thinking in effect sizes. J. Undergrad. Neurosci. Educ. 16, E21–E25. https://doi.org/10.31234/osf.io/zvm9a.

Calin-Jageman, R.J., Cumming, G., Greenland, S., Katz, P.S., Krafnick, A., Lakens, D., Mcshane, B., Peters, G.-J., Pliske, R., Wagen, E.-J., 2019. Estimation for better inference in neuroscience significance statement. eNeuro 6, 205–224.

Carbo-Gas, M., Vazquez-Sanroman, D., Aguirre-Manzo, L., Coria-Avila, G.A., Manzo, J., Sanchis-Segura, C., Miquel, M., 2014a. Involving the cerebellum in cocaine-induced memory: pattern of cFos expression in mice trained to acquire conditioned preference for cocaine. Addiction Biol. 19, 61–76. https://doi.org/10.1111/adb.12042.

Carbo-Gas, M., Vazquez-Sanroman, D., Gil-Miravet, I., De las Heras-Chanes, J., Coria-Avila, G.A., Manzo, J., Sanchis-Segura, C., Miquel, M., 2014b. Cerebellar hallmarks of conditioned preference for cocaine. Physiol. Behav. 132, 24–35. https://doi.org/10.1016/j.physbeh.2014.04.044.

Carbo-Gas, M., Moreno-Rius, J., Guarque-Chabrera, J., Vazquez-Sanroman, D., Gil-Miravet, I., Carulli, D., Hoebeek, F., De Zeeuw, C., Sanchis-Segura, C., Miquel, M., 2017. Cerebellar perineuronal nets in cocaine-induced pavlovian memory: site matters. Neuropharmacology 125, 166–180. https://doi.org/10.1016/j.neuropharm.2017.07.009.

Carta, I., Chen, C.H., Schott, A.L., Dorizan, S., Khodakhah, K., 2019. Cerebellar modulation of the reward circuitry and social behavior. Science 80, 363. https://doi.org/10.1126/science.aav0581 eaav0581.

Carulli, D., Rhodes, K.E., Brown, D.J., Bonnert, T.P., Pollack, S.J., Oliver, K., Strata, P., Fawcett, J.W., 2006. Composition of perineuronal nets in the adult rat cerebellum and the cellular origin of their components. J. Comp. Neurol. 494, 559–577. https://doi.org/10.1002/cne.20822.

Carulli, D., Broersen, R., de Winter, F., Muir, E.M., Meškovic, M., de Waal, M., de Vries, S., Boele, H.J., Canto, C.B., de Zeeuw, C.I., Verhaagen, J., 2020. Cerebellar plasticity and associative memories are controlled by perineuronal nets. Proc. Natl. Acad. Sci. U.S.A. 117, 6855–6865. https://doi.org/10.1073/pnas.1916163117.

Celio, M.R., Chiquet-Ehrismann, R., 1993. Perineuronal nets" around cortical interneurons expressing parvalbumin are rich in tenascin. Neurosci. Lett. 162, 137–140. https://doi.org/10.1016/0304-3940(93)90579-A.

Chen, C.H., Fremont, R., Arteaga-Bracho, E.E., Khodakhah, K., 2014. Short latency cerebellar modulation of the basal ganglia. Nat. Neurosci. 17 (12), 1767–1775. https://doi.org/10.1038/nn.3868.

Chen, H., He, D., Lasek, A.W., 2015. Repeated binge drinking increases perineuronal nets in the insular cortex. Alcohol Clin. Exp. Res. 39, 1930–1938. https://doi.org/10.1111/acer.12847.

Christensen, A.C., Lensjø, K.K., Lepperød, M.E., Dragly, S.A., Sutterud, H., Blackstad, J.S., Fyhn, M., Hafting, T., 2021. Perineuronal nets stabilize the grid cell network. Nat. Commun. 12, 1–17. https://doi.org/10.1038/s41467-020-20241-w.

Ciccarelli, A., Weijers, D., Kwan, W., Warner, C., Bourne, J., Gross, C.T., 2021. Sexually dimorphic perineuronal nets in the rodent and primate reproductive circuit. J. Comp. Neurol. 529, 3274–3291. https://doi.org/10.1002/cne.25167.

Cohen, J., 1988. Statistical Power Analisys for the Behavioral Sciences, second ed. Lawrence Earlbaum Associates, Publishers, New Yotk. https://doi.org/10.4324/9780203771587.

Coleman, L.G., Liu, W., Oguz, I., Styner, M., Crews, F.T., 2014. Adolescent binge ethanol treatment alters adult brain regional volumes, cortical extracellular matrix protein and behavioral flexibility. Pharmacol. Biochem. Behav. 116, 142–151. https://doi.org/10.1016/j.pbb.2013.11.021.

Corvetti, L., Rossi, F., 2005. Degradation of chondroitin sulfate proteoglycans induces sprouting of intact Purkinje axons in the cerebellum of the adult rat. J. Neurosci. 25, 7150–7158. https://doi.org/10.1523/JNEUROSCI.0683-05.2005.

Crook, J.D., Hendrickson, A., Erickson, A., Possin, D., Robinson, F.R., 2007. Purkinje cell axon collaterals terminate on Cat-301+ neurons in Macaca monkey cerebellum. Neuroscience 149, 834–844. https://doi.org/10.1016/j.neuroscience.2007.08.030.

Cumming, G., 2012. Understanding the New Statistics: Effect Sizes, Confidence Intervals, and Meta-Analysis, first ed. Routledge, New York, NY.

Cumming, G., Calin-Jageman, R., 2017. Introduction to the New Statistics: Estimation, Open Science, and beyond, first ed. Routledge, New York, NY.

Cumming, G., Maillardet, R., 2006. Confidence intervals and replication: where will the next mean fall? Psychol. Methods 11, 217–227. https://doi.org/10.1037/1082-989X.11.3.217.

Dauth, S., Grevesse, T., Pantazopoulos, H., Campbell, P.H., Maoz, B.M., Berretta, S., Parker, K.K., 2016. Extracellular matrix protein expression is brain region dependent. J. Comp. Neurol. 524, 1309–1336. https://doi.org/10.1002/cne.23965.

Deverett, B., Kislin, M., Tank, D.W., Wang, S.S.H., 2019. Cerebellar disruption impairs working memory during evidence accumulation. Nat. Commun. 10, 1–7. https://doi.org/10.1038/s41467-019-11050-x.

Dityatev, A., Bruckner, G., Dityateva, G., Grosche, J., Kleene, R., Schachner, M., 2007. Activity-dependent formation and functions of chondroitin sulfate-rich extracellular matrix of perineuronal nets. Dev. Neurobiol. 67, 570–588. https://doi.org/10.1002/dneu.20361.

Dumoulin, A., Triller, A., Dieudonné, S., 2001. IPSC kinetics at identified GABAergic and mixed GABAergic and glycinergic synapses onto cerebellar Golgi cells. J. Neurosci. 21, 6045–6057. https://doi.org/10.1523/jneurosci.21-16-06045.2001.

Dunsmoor, J.E., Niv, Y., Daw, N., Phelps, E.A., 2015. Rethinking extinction. Neuron 88, 47–63. https://doi.org/10.1016/j.neuron.2015.09.028.

D'Angelo, E., Rossi, P., Armano, S., Taglietti, V., 1999. Evidence for NMDA and mGLU receptor-dependent long-term potentiation of mossy fiber-granule cell transmission in rat cerebellum. J. Neurophysiol. 81, 277–287. https://doi.org/10.1152/jn.1999.81.1.277.

D'Angelo, E., Solinas, S., Mapelli, J., Gandolfi, D., Mapelli, L., Prestori, F., 2013. The cerebellar Golgi cell and spatiotemporal organization of granular layer activity. Front. Neural Circ. 7, 1–21. https://doi.org/10.3389/fncir.2013.00093.

Faissner, A., Pyka, M., Geissler, M., Sobik, T., Frischknecht, R., Gundelfinger, E.D., Seidenbecher, C., 2010. Contributions of astrocytes to synapse formation and maturation - potential functions of the perisynaptic extracellular matrix. Brain Res. Rev. 63, 26–38. https://doi.org/10.1016/j.brainresrev.2010.01.001.

Faul, F., Erdfelder, E., Lang, A.-G., Buchner, A., 2007. G*Power 3: a flexible statistical power analysis program for the social, behavioral, and biomedical sciences. Behav. Res. Methods 39, 175–191. https://doi.org/10.3758/bf03193146.

Ferrer-Ferrer, M., Dityatev, A., 2018. Shaping synapses by the neural extracellular matrix. Front. Neuroanat. 12, 1–16. https://doi.org/10.3389/fnana.2018.00040.

Forster, G.L., Blaha, C.D., 2003. Pedunculopontine tegmental stimulation evokes striatal dopamine efflux by activation of acetylcholine and glutamate receptors in the midbrain and pons of the rat. Eur. J. Neurosci. 17, 751–762. https://doi.org/10.1046/j.1460-9568.2003.02511.x.

Foscarin, S., Ponchione, D., Pajaj, E., Leto, K., Gawlak, M., Wilczynski, G.M., Rossi, F., Carulli, D., 2011. Experience-dependent plasticity and modulation of growth regulatory molecules at central synapses. PLoS One 6. https://doi.org/10.1371/journal.pone.0016666.

Fox, K., Caterson, B., 2002. Neuroscience: freeing the brain from the perineuronal net. Science 298 (80-), 1187–1189. https://doi.org/10.1126/science.1079224.

Frontera, J.L., Baba Aissa, H., Sala, R.W., Mailhes-Hamon, C., Georgescu, I.A., Léna, C., Popa, D., 2020. Bidirectional control of fear memories by cerebellar neurons projecting to the ventrolateral periaqueductal grey. Nat. Commun. 11, 1–17. https://doi.org/10.1038/s41467-020-18953-0.

Galliano, E., Mazzarello, P., D'Angelo, E., 2010. Discovery and rediscoveries of Golgi cells. J. Physiol. 588, 3639–3655. https://doi.org/10.1113/jphysiol.2010.189605.

Giamanco, K.A., Matthews, R.T., 2012. Deconstructing the perineuronal net: cellular contributions and molecular composition of the neuronal extracellular matrix. Neuroscience 218, 367–384. https://doi.org/10.1016/j.neuroscience.2012.05.055.

Gil-Miravet, I., Guarque-Chabrera, J., Carbo-Gas, M., Olucha-Bordonau, F., Miquel, M., 2019. The role of the cerebellum in drug-cue associative memory: functional interactions with the medial prefrontal cortex. Eur. J. Neurosci. 50 https://doi.org/10.1111/ejn.14187.

Gil-Miravet, I., Melchor-Eixea, I., Arias-Sandoval, E., Vasquez-Celaya, L., Guarque-Chabrera, J., Olucha-Bordonau, F., Miquel, M., 2021. From back to front: a functional model for the cerebellar modulation in the establishment of conditioned

preferences for cocaine-related cues. Addiction Biol. 26 https://doi.org/10.1111/adb.12834.
Gildawie, K.R., Honeycutt, J.A., Brenhouse, H.C., 2020. Region-specific effects of maternal separation on perineuronal net and parvalbumin-expressing interneuron formation in male and female rats. Neuroscience 428, 23–37. https://doi.org/10.1016/j.neuroscience.2019.12.010.
Greenland, S., Senn, S.J., Rothman, K.J., Carlin, J.B., Poole, C., Goodman, S.N., Altman, D.G., 2016. Statistical tests, P values, confidence intervals, and power: a guide to misinterpretations. Eur. J. Epidemiol. 31, 337–350. https://doi.org/10.1007/s10654-016-0149-3.
Guadagno, A., Verlezza, S., Long, H., Wong, T.P., Walker, C.D., 2020. It is all in the right amygdala: increased synaptic plasticity and perineuronal nets in male, but not female, juvenile rat pups after exposure to early-life stress. J. Neurosci. 40, 8276–8291. https://doi.org/10.1523/JNEUROSCI.1029-20.2020.
Guarque-Chabrera, J., Gil-Miravet, I., Olucha-Bordonau, F., Melchor-Eixea, I., Miquel, M., 2022. When the front fails, the rear wins. Cerebellar correlates of prefrontal dysfunction in cocaine-induced memory in male rats. Prog. Neuro Psychopharmacol. Biol. Psychiatr. 112, 110429 https://doi.org/10.1016/j.pnpbp.2021.110429.
Hartig, W., Brauer, K., Bruckner, G., 1992. Wisteria floribunda agglutinin-labelled nets surround parvalbumin-containing neurons. Neuroreport 3, 869–872. https://doi.org/10.1097/00001756-199210000-00012.
Ho, J., Tumkaya, T., Aryal, S., Choi, H., Claridge-Chang, A., 2019. Moving beyond P values: data analysis with estimation graphics. Nat. Methods 16, 565–566. https://doi.org/10.1038/s41592-019-0470-3.
Jorgensen, E.T., Gonzalez, A.E., Harkness, J.H., Hegarty, D.M., Thakar, A., Burchi, D.J., Aadland, J.A., Aicher, S.A., Sorg, B.A., Brown, T.E., 2020. Cocaine memory reactivation induces functional adaptations within parvalbumin interneurons in the rat medial prefrontal cortex. Addiction Biol. 1–11 https://doi.org/10.1111/adb.12947.
Kassambara, A., 2021. Rstatix: Pipe-Friendly Framework for Basic Statistical Tests.
Kilkenny, C., Browne, W.J., Cuthill, I.C., Emerson, M., Altman, D.G., 2010. Improving bioscience research reporting: the arrive guidelines for reporting animal research. PLoS Biol. 8, 6–10. https://doi.org/10.1371/journal.pbio.1000412.
Kosaka, T., Heizmann, C.W., 1989. Selective staining of a population of parvalbumin-containing GABAergic neurons in the rat cerebral cortex by lectins with specific affinity for terminal N-acetylgalactosamine. Brain Res. 483, 158–163. https://doi.org/10.1016/0006-8993(89)90048-6.
Kostadinov, D., Häusser, M., 2022. Reward signals in the cerebellum: origins, targets, and functional implications. Neuron 110, 1290–1303. https://doi.org/10.1016/j.neuron.2022.02.015.
Lasek, A.W., Chen, H., Chen, W.Y., 2018. Releasing addiction memories trapped in perineuronal nets. Trends Genet. 34, 197–208. https://doi.org/10.1016/j.tig.2017.12.004.
Lensjø, K.K., Christensen, A.C., Tennøe, S., Fyhn, M., Hafting, T., 2017a. Differential expression and cell-type specificity of perineuronal nets in hippocampus, medial entorhinal cortex, and visual cortex examined in the rat and mouse. eNeuro 4. https://doi.org/10.1523/ENEURO.0379-16.2017.
Lensjø, K.K., Lepperød, M.E., Dick, G., Hafting, T., Fyhn, M., 2017b. Removal of perineuronal nets unlocks juvenile plasticity through network mechanisms of decreased inhibition and increased gamma activity. J. Neurosci. 37, 1269–1283. https://doi.org/10.1523/JNEUROSCI.2504-16.2016.
Mangiafico, Salvatore, 2022. Rcompanion: Functions to Support Extension Education Program Evaluation. R package version 2.4.13. https://CRAN.R-project.org/package=rcompanion.
Mascio, G., Notartomaso, S., Martinello, K., Liberatore, F., Bucci, D., Imbriglio, T., Cannella, M., Antenucci, N., Scarselli, P., Lattanzi, R., Bruno, V., Nicoletti, F., Fucile, S., Battaglia, G., 2022. A progressive build-up of perineuronal nets in the somatosensory cortex is associated with the development of chronic pain in mice. J. Neurosci. 42, 3037–3048. https://doi.org/10.1523/jneurosci.1714-21.2022.
Miao, C., Cao, Q., Moser, M.B., Moser, E.I., 2017. Parvalbumin and somatostatin interneurons control different space-coding networks in the medial entorhinal cortex. Cell 171, 507–521. https://doi.org/10.1016/j.cell.2017.08.050 e17.
Michel, M.C., Murphy, T.J., Motulsky, H.J., 2020. New author guidelines for displaying data and reporting data analysis and statistical methods in experimental biology. Mol. Pharmacol. 97, 49–60. https://doi.org/10.1124/mol.119.118927.
Miquel, M., Nicola, S.M., Gil-Miravet, I., Guarque-Chabrera, J., Sanchez-Hernandez, A., 2019. A working hypothesis for the role of the cerebellum in impulsivity and compulsivity. Front. Behav. Neurosci. 13 https://doi.org/10.3389/fnbeh.2019.00099.
Morawski, M., Brückner, M.K., Riederer, P., Brückner, G., Arendt, T., 2004. Perineuronal nets potentially protect against oxidative stress. Exp. Neurol. 188, 309–315. https://doi.org/10.1016/j.expneurol.2004.04.017.
Moreno-Rius, J., Miquel, M., 2017. The cerebellum in drug craving. Drug Alcohol Depend. 173, 151–158. https://doi.org/10.1016/j.drugalcdep.2016.12.028.
Morikawa, S., Ikegaya, Y., Narita, M., Tamura, H., 2017. Activation of perineuronal net-expressing excitatory neurons during associative memory encoding and retrieval. Sci. Rep. 7, 1–9. https://doi.org/10.1038/srep46024.
Moulton, E.A., Elman, I., Becerra, L.R., Goldstein, R.Z., Borsook, D., 2014. The cerebellum and addiction: insights gained from neuroimaging research. Addiction Biol. 19, 317–331. https://doi.org/10.1111/adb.12101.
Nuzzo, R., 2014. Scientific method: statistical errors. Nature 506, 150–152. https://doi.org/10.1038/506150a.
Palay, S.L., Chan-Palay, V., 1974. Cerebellar Cortex. Cytology and Organization, Cerebellar Cortex. Cytology and Organization. Springer-Verlag, Berlin. https://doi.org/10.1007/978-3-642-65581-4.
Pastore, M., 2018. Overlapping: a R package for estimating overlapping in empirical distributions. J. Open Source Softw. 3, 1023. https://doi.org/10.21105/joss.01023.
Pastore, M., Calcagnì, A., 2019. Measuring distribution similarities between samples: a distribution-free overlapping index. Front. Psychol. 10, 1–8. https://doi.org/10.3389/fpsyg.2019.01089.
Paxinos, G., Watson, C., 1998. The Rat Brain in Stereotaxic Coordinates, fourth ed. Academic Press Inc., San Diego.
Percie du Sert, N., Ahluwalia, A., Alam, S., Avey, M.T., Baker, M., Browne, W.J., Clark, A., Cuthill, I.C., Dirnagl, U., Emerson, M., Garner, P., Holgate, S.T., Howells, D.W., Hurst, V., Karp, N.A., Lazic, S.E., Lidster, K., MacCallum, C.J., Macleod, M., Pearl, E.J., Petersen, O.H., Rawle, F., Reynolds, P., Rooney, K., Sena, E.S., Silberberg, S.D., Steckler, T., Würbel, H., 2020a. Reporting Animal Research: Explanation and Elaboration for the Arrive Guidelines 2.0. PLoS Biology. https://doi.org/10.1371/journal.pbio.3000411.
Percie du Sert, N., Hurst, V., Ahluwalia, A., Alam, S., Avey, M.T., Baker, M., Browne, W.J., Clark, A., Cuthill, I.C., Dirnagl, U., Emerson, M., Garner, P., Holgate, S.T., Howells, D.W., Karp, N.A., Lazic, S.E., Lidster, K., MacCallum, C.J., Macleod, M., Pearl, E.J., Petersen, O.H., Rawle, F., Reynolds, P., Rooney, K., Sena, E.S., Silberberg, S.D., Steckler, T., Würbel, H., 2020b. The arrive guidelines 2.0: updated guidelines for reporting animal research. PLoS Biol. 18, 1–12. https://doi.org/10.1371/journal.pbio.3000410.
Pizzorusso, T., Medini, P., Berardi, N., Chierzi, S., Fawcett, J.W., Maffei, L., 2002. Reactivation of ocular dominance plasticity in the adult visual cortex. Science 298 (80-), 1248–1251. https://doi.org/10.1126/science.1072699.
Prabhakar, V., Raman, R., Capila, I., Bosques, C.J., Pojasek, K., Sasisekharan, R., 2005. Biochemical characterization of the chondroitinase ABC I active site. Biochem. J. 390, 395–405. https://doi.org/10.1042/BJ20050532.
Prestori, F., Mapelli, L., D'Angelo, E., 2019. Diverse neuron properties and complex network dynamics in the cerebellar cortical inhibitory circuit. Front. Mol. Neurosci. 12, 1–23. https://doi.org/10.3389/fnmol.2019.00267.
Pruim, R., Kaplan, D.T., Horton, N.J., 2017. The mosaic package: helping students to "think with data" using. R. R J. 9, 77–102. https://doi.org/10.32614/rj-2017-024.
R Core Team, 2021. R: A Language and Environment for Statistical Computing. R Foundation for Statistical Computing, Vienna, Austria. URL. https://www.R-project.org/.
Roura-Martínez, D., Díaz-Bejarano, P., Ucha, M., Paiva, R.R., Ambrosio, E., Higuera-Matas, A., 2020. Comparative analysis of the modulation of perineuronal nets in the prefrontal cortex of rats during protracted withdrawal from cocaine, heroin and sucrose self-administration. Neuropharmacology 180, 108290. https://doi.org/10.1016/j.neuropharm.2020.108290.
Rousselet, G.A., Pernet, C.R., Wilcox, R.R., 2017. Beyond differences in means: robust graphical methods to compare two groups in neuroscience. Eur. J. Neurosci. 46, 1738–1748. https://doi.org/10.1111/ejn.13610.
Ruscio, J., 2008. A probability-based measure of effect size: robustness to base rates and other factors. Psychol. Methods 13, 19–30. https://doi.org/10.1037/1082-989X.13.1.19.
Sacchetti, B., Scelfo, B., Strata, P., 2005. The cerebellum: synaptic changes and fear conditioning. Neuroscientist 11, 217–227. https://doi.org/10.1177/1073858405276428.
Sakoori, K., Murphy, N.P., 2005. Maintenance of conditioned place preferences and aversion in C57BL6 mice: effects of repeated and drug state testing. Behav. Brain Res. 160, 34–43. https://doi.org/10.1016/j.bbr.2004.11.013.
Sanchez-Hernandez, A., Nicolas, C., Gil-Miravet, I., Guarque-Chabrera, J., Solinas, M., Miquel, M., 2021. Time-dependent regulation of perineuronal nets in the cerebellar cortex during abstinence of cocaine-self administration. Psychopharmacology (Berl) 238 (4), 1059–1068. https://doi.org/10.1007/s00213-020-05752-0.
Schindelin, J., Arganda-Carreras, I., Frise, E., Kaynig, V., Longair, M., Pietzsch, T., Preibisch, S., Rueden, C., Saalfeld, S., Schmid, B., Tinevez, J.Y., White, D.J., Hartenstein, V., Eliceiri, K., Tomancak, P., Cardona, A., 2012. Fiji: an open-source platform for biological-image analysis. Nat. Methods 9, 676–682. https://doi.org/10.1038/nmeth.2019.
Slaker, M., Churchill, L., Todd, R.P., Blacktop, J.M., Zuloaga, D.G., Raber, J., Darling, R.A., Brown, T.E., Sorg, B.A., 2015. Removal of perineuronal nets in the medial prefrontal cortex impairs the acquisition and reconsolidation of a cocaine-induced conditioned place preference memory. J. Neurosci. 35, 4190–4202. https://doi.org/10.1523/JNEUROSCI.3592-14.2015.
Slaker, M., Blacktop, J.M., Sorg, B.A., 2016. Caught in the net: perineuronal nets and addiction. Neural Plast. 7538208 https://doi.org/10.1155/2016/7538208, 2016.
Sorg, B.A., Berretta, S., Blacktop, J.M., Fawcett, J.W., Kitagawa, H., Kwok, J.C.F., Miquel, M., 2016. Casting a wide net: role of perineuronal nets in neural plasticity. J. Neurosci. 36, 11459–11468. https://doi.org/10.1523/JNEUROSCI.2351-16.2016.
Sotelo, C., Llinás, R., 1972. Specialized membrane junctions between neurons in the vertebrate cerebellar cortex. J. Cell Biol. 53, 271–289. https://doi.org/10.1083/jcb.53.2.271.
Tabuchi, S., Gilmer, J.I., Purba, K., Person, A.L., 2018. Pathway specific drive of cerebellar Golgi cells reveals integrative rules of cortical inhibition. J. Neurosci. 39, 1169–1181. https://doi.org/10.1101/356378.
Traver, V.J., Pla, F., Miquel, M., Carbo-Gas, M., Gil-Miravet, I., Guarque-Chabrera, J., 2019. Cocaine-induced preference conditioning: a machine vision perspective. Neuroinformatics 17. https://doi.org/10.1007/s12021-018-9401-1.
Van Den Oever, M.C., Lubbers, B.R., Goriounova, N.A., Li, K.W., Van Der Schors, R.C., Loos, M., Riga, D., Wiskerke, J., Binnekade, R., Stegeman, M., Schoffelmeer, A.N.M., Mansvelder, H.D., Smit, A.B., De Vries, T.J., Spijker, S., 2010. Extracellular matrix plasticity and GABAergic inhibition of prefrontal cortex pyramidal cells facilitates relapse to heroin seeking. Neuropsychopharmacology 35, 2120–2133. https://doi.org/10.1038/npp.2010.90.

Vazquez-Sanroman, D., Carbo-Gas, M., Leto, K., Cerezo-Garcia, M., Gil-Miravet, I., Sanchis-Segura, C., Carulli, D., Rossi, F., Miquel, M., 2015a. Cocaine-induced plasticity in the cerebellum of sensitised mice. Psychopharmacology (Berl) 232, 4455–4467. https://doi.org/10.1007/s00213-015-4072-1.

Vazquez-Sanroman, D., Leto, K., Cerezo-Garcia, M., Carbo-Gas, M., Sanchis-Segura, C., Carulli, D., Rossi, F., Miquel, M., 2015b. The cerebellum on cocaine: plasticity and metaplasticity. Addict. Biol. 20, 941–955. https://doi.org/10.1111/adb.12223.

Vazquez-Sanroman, D.B., Monje, R.D., Bardo, M.T., 2017. Nicotine self-administration remodels perineuronal nets in ventral tegmental area and orbitofrontal cortex in adult male rats. Addiction Biol. 22, 1743–1755. https://doi.org/10.1111/adb.12437.

Wagner, M.J., Kim, T.H., Savall, J., Schnitzer, M.J., Luo, L., 2017. Cerebellar granule cells encode the expectation of reward. Nature 544, 96–100. https://doi.org/10.1038/nature21726.

Wang, D., Fawcett, J., 2012. The perineuronal net and the control of cns plasticity. Cell Tissue Res. 349, 147–160. https://doi.org/10.1007/s00441-012-1375-y.

Wasserstein, R.L., Lazar, N.A., 2016. The ASA's statement on p-values: context, process, and purpose. Am. Statistician 70, 129–133. https://doi.org/10.1080/00031305.2016.1154108.

Wegner, F., Härtig, W., Bringmann, A., Grosche, J., Wohlfarth, K., Zuschratter, W., Brückner, G., 2003. Diffuse perineuronal nets and modified pyramidal cells immunoreactive for glutamate and the GABAA receptor α1 subunit form a unique entity in rat cerebral cortex. Exp. Neurol. 184, 705–714. https://doi.org/10.1016/S0014-4886(03)00313-3.

Womersley, J.S., Townsend, D.M., Kalivas, P.W., Uys, J.D., 2019. Targeting redox regulation to treat substance use disorder using N-acetylcysteine. Eur. J. Neurosci. 50, 2538–2551. https://doi.org/10.1111/ejn.14130.

Xue, Y.X., Xue, L.F., Liu, J.F., He, J., Deng, J.H., Sun, S.C., Han, H. Bin, Luo, Y.X., Xu, L. Z., Wu, P., Lu, L., 2014. Depletion of perineuronal nets in the amygdala to enhance the erasure of drug memories. J. Neurosci. 34, 6647–6658. https://doi.org/10.1523/JNEUROSCI.5390-13.2014.

Zingg, B., Peng, B., Huang, J., Tao, H.W., Zhang, L.I., 2020. Synaptic specificity and application of anterograde transsynaptic AAV for probing neural circuitry. J. Neurosci. 40, 3250–3267. https://doi.org/10.1523/JNEUROSCI.2158-19.2020.